Fig. 3 (continued)

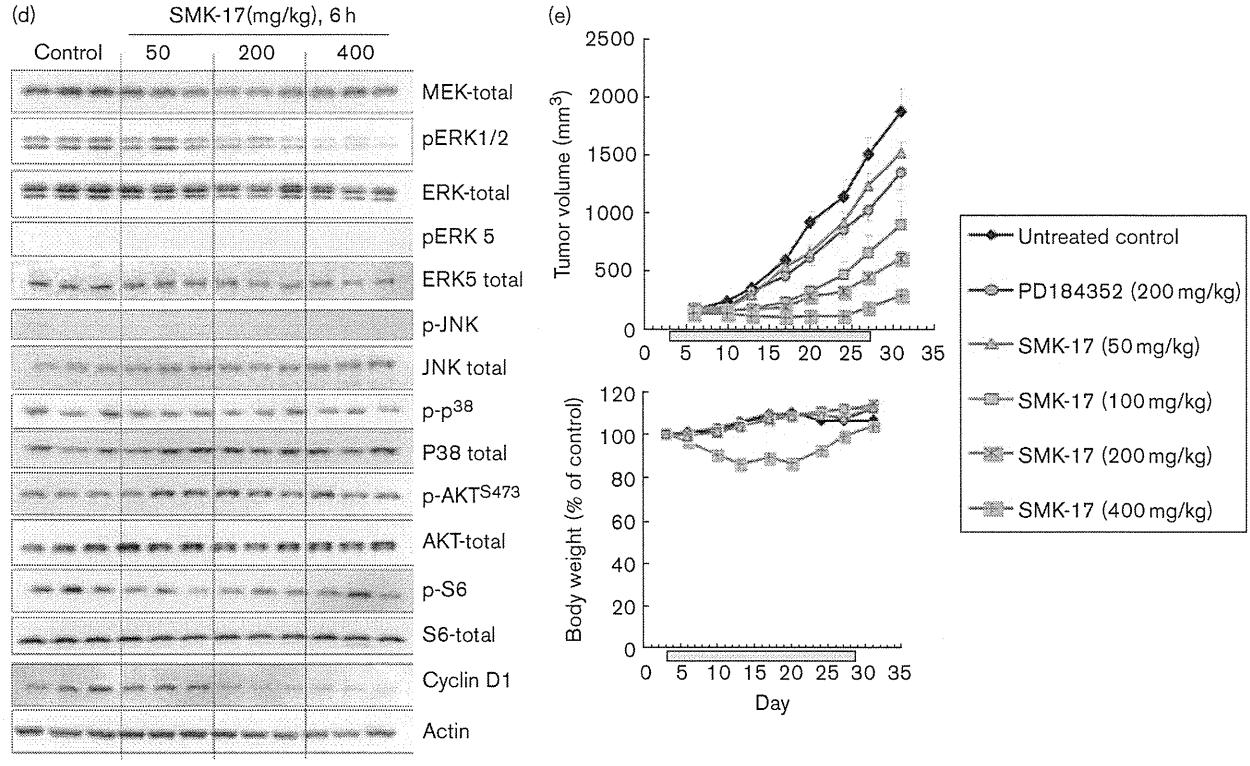

position of R1, which is adopted in compounds 11–19, was the favorable structure for both cell-free and cell-based MEK inhibition. In contrast, hydroxy-terminal substituents such as in compounds 2, 7–10, and 20 were unfavorable. In particular, an isopropyl-amine at the fourth position (SMK-17) was the optimal structure for both intracellular and cell-free MEK1 kinase inhibition.

A low *c* Log *D*, which predicts high water solubility, is required for in-vivo exposure of orally administered drugs. The *c* Log *D* of compound 1 is 3.95 and the solubility in JP-2 (pH 6.8) buffer is less than 0.5 μmol/l. Alkyl-amine-adopted derivatives (compounds 3–6, 11–19) achieved a lower *c* Log *D* and a higher water solubility in the range of 61–88 μmol/l in JP-2 solution, compared with the piperidinol series (compounds 2, 7–10), in addition to improvement in in-vitro activities. Adoption of a basic residue such as alkyl-amine in the R1 position is considered to contribute to the improvement of the polar nature and high aqueous solubility.

We observed two significant structure–activity relationships in the compound's optimization. First, substitution of alkyl-amine, especially an isopropyl-amine, at the R1 position yielded better profiles of both aqueous solubility and in-vitro activities. A comparison between the cell-based MEK inhibitory potencies of compound 9 and its isopropyl-amine analog (SMK-17) revealed an eight-fold improvement. The second critical finding was that a substituent for chlorine was desirable at the R2 position rather than for fluorine or methyl. Substitution of chlorine for fluorine at the R2 position of compound 16 results in a four-fold increase in the intracellular MEK inhibition of SMK-17. The same substitution in the piperidinol pair (analogs 8 and 9) provides an approximately three-fold improvement in cell potency. The two structure–activity relationships advance providing the benefit of improved aqueous solubility and in-vitro activity. We finally obtained SMK-17, which has a more than 100-fold aqueous solubility in JP-2 and 11-fold strengthened MEK kinase inhibition.

Binding mode to MEK1

To understand the characteristics of these derivatives, we built a docking model of SMK-17 and MEK1 (Fig. 1a). The predicted binding model showed that SMK-17 binds to an allosteric pocket adjacent to the ATP-binding site similar to U0126 or PD325089 [18], which indicates that SMK-17 is a non-ATP-competitive inhibitor. In addition, the protonated amine of the alkyl-amine group at the R1 forms salt bridges with the γ phosphate of ATP. The aliphatic carbons of the alkyl-amine substituent have hydrophobic interactions with M219 and V224 (not shown in this figure) in the activation segment. This predicted binding mode supports the structure–activity relationship that inhibitory activity is well correlated with the size of the alkyl-amine as shown in Table 2.

ATP dependency of kinase inhibition

To confirm the allosteric binding characteristic of SMK-17 predicted in Fig. 1a, we examined the ATP dependence of MEK1 inhibition by SMK-17 and tested MEK1 kinase inhibition at various concentrations of ATP from 10 to 1000 μmol/l (Fig. 1b). The ATP concentration was found to have little effect on the MEK1 inhibition of SMK-17. IC_{50} values of SMK-17 for MEK1 kinase were 31.4 (ATP 10 μmol/l), 36.6 (100 μmol/l), and 36.5 nmol/l (1000 μmol/l) respectively. Thus, SMK-17 was regarded as a non-ATP-competitive inhibitor of MEK1. These results coincide with the prediction by the in-silico binding model that SMK-17 does not exclude ATP from MEK1.

Kinase inhibitory selectivity

SMK-17 was further characterized for its kinase selectivity with Millipore's kinase profiler. The screen of 233 protein kinases incubated with 1000 nmol/l of this compound has been described in Supplement 4. Figure 1c shows the top 40 kinases, which were inhibited by SMK-17. MEK1 was the kinase most sensitive to SMK-17, and was inhibited by 74%. There was no significant (> 50%) inhibition of any other protein kinases observed except for MEK1. Notably, SMK-17 had little effect on MEK1 isoforms, such as MKK4 (29% inhibition), MKK6 (2%), and MKK7 (32%). The non-ATP-competitive but allosteric binding mode of this compound probably contributes to its high selectivity to MEK1/2.

Despite their allosteric inhibition mode, PD184352 and U0126 were previously reported to inhibit MKK5 as an off-target [19]. It is supposed that the conformation of the allosteric pocket of MEK1/2 is similar to that of MKK5. However, SMK-17 did not inhibit ERK5 phosphorylation, which is a substrate of MKK5 in both cell-based and in-vivo experiments (Fig. 3d and Supplement 1). These results indicated that SMK-17 is a non-ATP-competitive and highly selective kinase inhibitor of MEK1/2.

Intracellular MEK and growth inhibition

To further investigate the intracellular effects of SMK-17, the antiproliferative effect of SMK-17 was examined against murine colorectal cancer colon 26, human colorectal cancer HT-29, human pancreas cancer Panc-1, and human prostate cancer LNCaP. SMK-17 was active in suppressing cell growth in colon 26 and HT-29 cell lines, which harbor highly phosphorylated MEK1/2 and ERK1/2. The GI_{50} values were 2.0 and 0.34 μmol/l, respectively (Fig. 2a). In contrast, SMK-17 was not effective in tumor cells, which do not have highly phosphorylated MEK1/2 and ERK1/2, such as Panc-1 and LNCaP cells. As reported previously with the other MEK inhibitors [20], SMK-17 is highly effective in suppressing the proliferation of tumor cells with aberrant activated MAPK pathway signaling, which is reflected by the phosphorylation levels of MEK1/2 and ERK1/2.

To understand the underlying mechanism of SMK-17 activity on cancer cell proliferation, we analyzed its effect on the cell cycle progression and cyclin D1 expression in tumor cells. In responsive cell lines, colon 26 and HT-29 colorectal cancer cells, inhibition of ERK1/2 phosphorylation by SMK-17 led to a G1 phase cell cycle arrest at an approximately five-fold concentration of GI_{50}, 10 μmol/l in HT-29 and 1 μmol/l in colon 26 (Fig. 2b and c), which were similar to the effects of PD184352. Correspondingly, treatment with SMK-17 resulted in the downregulation of cyclin D1, a key cell cycle regulator for G1–S phase progression, which is a typical physiological effect of MEK1/2 inhibitors [10]. It was reported that cyclin D1 is an unstable protein, with a half-life of approximately 30 min [21]. The amount of cyclin D1 protein decreased 8–16 h after MEK was inhibited. The time-lagged response of cyclin D1 decrease can be explained by two independent regulatory mechanisms of cyclin D1. First, protein synthesis of cyclin D1 can be translated from the remaining mRNA. The translation of cyclin D1 does not stop briefly, although the MEK inhibitor suppresses MEK-ERK-inducing cyclin D1 transcription activity. Second, phosphorylation of cyclin D1 at T286 by ERK enhances its ubiquitination and proteasomal degradation [22]. Hence, inhibition of MEK-ERK attenuates the phosphorylation of T286 and the degradation of cyclin D1 protein. Accordingly, inhibition of MEK-ERK results in a slow decrease in cyclin D1. A negative feedback mechanism by ERK, which suppresses upstream of the ras/raf signal pathway, has been reported in the previous study [23]. In this report, we observed an increased phosphorylation of MEK by SMK-17 in HT-29 cells. As the MEK inhibitor suppressed the activity of ERK including the negative feedback pathway, SMK-17 was likely to cause increased MEK1/2 phosphorylation by inactivating the negative feedback mechanism.

In contrast, in resistant Panc-1 and LNCaP cells, SMK-17 at the concentration of 30 μmol/l did not lead to marked G1 phase arrest and downregulation of cyclin D1 (Fig. 2d and Supplement 5). It is possible that proliferation of resistant cell lines is independent of MEK/MAPK pathway because these cell lines have phosphorylated S473 of AKT, which represents PI3K/AKT pathway activation (Fig. 2a). PI3K-dependent growth of Panc-1 cells are supported by several reports [24–26]. Our results support the PI3K pathway-dependent growth of MEK inhibitor-resistant cell lines. Furthermore, SMK-17 did not induce apoptosis, as evidenced by the sub-G1 population on flow cytometry analysis in all four cell lines, even under conditions of complete MEK inhibition (e.g. 10 μmol/l of SMK-17 on HT-29 cells). We confirmed that SMK-17 did not induce apoptosis in these cell lines, which were monitored with AnnexinV-APC and 7AAD double staining (data not shown). These results indicated that inhibition

of MEK/ERK signal pathway is not sufficient to induce apoptosis in all four cell lines.

To examine whether MEK inhibition of SMK-17 affects cell cycle arrest directly, we investigated the dose correlation between cell cycle arrest and intracellular MEK inhibition. As a result, an inverse correlation was observed between the intensity of ERK phosphorylation and an increase in the G1 population (Fig. 2e). Moreover, SMK-17 selectively inhibited Raf/MEK/ERK pathway activity in cells while having no effect on the activation status of other closely related intracellular signaling molecules such as ERK5, p38, JNK, and AKT (Supplement 1). These results indicated that SMK-17 induced G1 arrest through intracellular MEK1/2 inhibition as an on-target effect.

In-vivo antitumor activity

We evaluated the in-vivo efficacy of SMK-17 using the murine colorectal colon 26 cell syngeneic model in CDF1 mice. Colon 26 cells have a constitutively active K-ras mutation. After a single oral dose of SMK-17, tumors were excised at various time points after dosing and the tumor lysates were analyzed for phospho-ERK1/2 and total ERK levels. SMK-17 decreased the phospho-ERK1/2 level in the tumor mass after 50 mg/kg administration for 6 h. Treatment using 200 mg/kg caused a 24-h inhibition of phospho-ERK1/2 (Fig. 3a and Supplement 2 as quantification data).

The antitumor activity of SMK-17 was evaluated in the same model in CDF1 mice. When SMK-17 was administered to mice once daily at doses of 50 and 200 mg/kg, the antitumor activity was observed, from partial tumor growth inhibition at doses of 50 mg/kg to complete inhibition at 200 mg/kg (Fig. 3c) without significant body weight loss. In this experiment, PD184352 as a reference also showed tumor growth inhibition. In this syngeneic graft model, blood samples were collected from animals and the drug concentration in the plasma was measured for pharmacokinetic and pharmacodynamic analyses. SMK-17 concentrations in the plasma of mice are shown in Fig. 3b. Complete inhibition of ERK phosphorylation in tumors was achieved when the plasma drug concentration was more than 0.83 μg/ml (comparable to 1.4 μmol/l, $M_w = 584.8$). This minimum effective plasma concentration is similar to the GI_{50} value of colon 26 cells *in vitro*. Administration of 200 mg/kg of SMK-17, at which complete inhibition of intratumor MEK for 24 h per dosing occurs, caused complete inhibition of tumor growth. These results indicated that continuous exposure of SMK-17 was necessary for long-lasting inhibition of intratumor MEK1/2 and complete tumor growth inhibition in an animal model.

Furthermore, we evaluated the in-vivo pharmacodynamic study on SMK-17 against the HT-29 human tumor xenograft model (Fig. 3d). In this model, SMK-17 showed a dose-dependent phospho-ERK inhibition and cyclin D1 reduction in tumors 6 h after administration, similar to in-vitro results. Figure 3d shows that significant effects on the other signals except for ERK1/2 were not observed up to 400 mg/kg (e.g. phosphorylation S473 of AKT, S6, and the other MAPKs). It is suggested that SMK-17 selectively inhibited Raf/MEK/ERK pathway activity in the xenograft model. Exposure of SMK-17 in this animal model was similar to that in the colon 26 CDF1 mice model (Supplement 3). No difference in pharmacokinetics between nude mice and CDF1 mice was observed. We evaluated the antitumor activity of SMK-17 against this xenograft model. SMK-17 was orally administered daily at a dose range of 50–400 mg/kg in tumor-bearing mice for 25 days and it showed statistically significant tumor growth inhibition in a dose-dependent manner (Fig. 3e). In this study, partial tumor growth inhibition was observed at doses between 50 and 200 mg/kg, and complete inhibition was observed at 400 mg/kg. No notable adverse effects were observed in this study.

Conclusion

In conclusion, we found a very potent MEK inhibitor, SMK-17, from our structure–activity correlation study of the new derivative series of diphenyl amine sulfonamides. Kinase profiler and kinetic studies revealed that SMK-17 is a non-ATP-competitive and highly selective MEK1/2 inhibitor. Moreover, SMK-17 exhibited potent antitumor activity in animal models by oral administration. SMK-17 selectively blocked the MAPK pathway signaling without affecting other signal pathways both *in vitro* and *in vivo*. These findings suggest that SMK-17 is a useful chemical biology tool for characterizing the function of MEK/MAPK signaling both *in vitro* and *in vivo*.

Acknowledgements

We would like to thank Dr Kenichi Wakita for critical reading of the manuscript. We would also like to thank Dr Tohru Takashi and Dr Koichi Akahane for continuous encouragement in conducting these studies.

Conflicts of interest

There are no conflicts of interest.

References

1 Dalby KN, Morrice N, Caudwell FB, Avruch J, Cohen P. Identification of regulatory phosphorylation sites in mitogen-activated protein kinase (MAPK)-activated protein kinase-1a/p90rsk that are inducible by MAPK. *J Biol Chem* 1998; **273**:1496–1505. *http://www.ncbi.nlm.nih.gov/pubmed/9430688.*

2 Marais R, Wynne J, Treisman R. The SRF accessory protein Elk-1 contains a growth factor-regulated transcriptional activation domain. *Cell* 1993; **73**:381–393. *http://www.ncbi.nlm.nih.gov/pubmed/8386592.*

3 Sebolt-Leopold JS, Herrera R. Targeting the mitogen-activated protein kinase cascade to treat cancer. *Nat Rev Cancer* 2004; **12**:937–947. *http://www.ncbi.nlm.nih.gov/pubmed/15573115, http://www.nature.com/nrc/journal/v4/n12/full/nrc1503.html.*

4 Bos JL. Ras oncogenes in human cancer. *Cancer Res* 1990; **50**:1352. *http://www.ncbi.nlm.nih.gov/pubmed/2547513, http://cancerres.aacrjournals.*

org/content/49/17/4682.abstract?ijkey=332fc8fd82a5e0c5b13dc693262953e7ccddd4f1&keytype2=tf_ipsecsha.

5 Davies H, Bignell GR, Cox C, Stephens P, Edkins S, Futreal PA, *et al.* Mutations of the BRAF gene in human cancer. *Nature* 2002; **417**:949–954. *http://www.ncbi.nlm.nih.gov/pubmed/12068308?dopt=Abstract.*

6 Cohen Y, Xing M, Mambo E, Guo Z, Wu G, Sidransky D, *et al.* BRAF mutation in papillary thyroid carcinoma. *J Natl Cancer Inst* 2003; **95**:625–627. *http://www.ncbi.nlm.nih.gov/pubmed/12697856 http://jnci.oxfordjournals.org/content/95/8/625.abstract?ijkey=da94f758df955accebe5e60e4aa34896bf2dae22&keytype2=tf_ipsecsha.*

7 Cowley S, Paterson H, Kemp P, Marshall CJ. Activation of MAP kinase kinase is necessary and sufficient for PC12 differentiation and for transformation of NIH 3T3 cells. *Cell* 1994; **77**:841–852. *http://www.cell.com/retrieve/pii/0092867494901333.*

8 Mansour SJ, Matten WT, Hermann AS, Candia JM, Rong S, Ahn NG, *et al.* Transformation of mammalian cells by constitutively active MAP kinase kinase. *Science* 1994; **265**:966–970. *http://www.ncbi.nlm.nih.gov/pubmed/8052857, http://www.sciencemag.org/content/265/5174/966.abstract?ijkey=d4d45ca3cd0ae4da25d4d2391f3db8d265c7732f&keytype2=tf_ipsecsha.*

9 Sebolt-Leopold JS. MEK inhibitors: a therapeutic approach to targeting the Ras-MAP kinase pathway in tumors. *Curr Pharm Des* 2004; **10**: 1907–1914. *http://www.ncbi.nlm.nih.gov/pubmed/15180527.*

10 Roberts PJ, Der CJ. Targeting the Raf-MEK-ERK mitogen-activated protein kinase cascade for the treatment of cancer. *Oncogene* 2007; **26**:3291–3310. *http://www.nature.com/onc/journal/v26/n22/full/1210422a.html.*

11 Chiappori AA, Ellis PM, Hamm JT, Bitran JD, Eiseman I, Zinner RG, *et al.* Multicenter phase II study of the oral MEK inhibitor, CI-1040, in patients with advanced non-small-cell lung, breast, colon, and pancreatic cancer. *J Clin Oncol* 2004; **22**:4456–4462. *http://www.ncbi.nlm.nih.gov/pubmed/15483017.*

12 Lorusso P, Krishnamurthi S, Rinehart JR, Nabell L, Croghan G, Meyer MB, *et al.* A phase 1-2 clinical study of a second generation oral MEK inhibitor, PD 0325901 in patients with advanced cancer. *J Clin Oncol* 2005; **23**:3006. *http://meeting.ascopubs.org/cgi/content/abstract/23/16_suppl/3011.*

13 LoRusso P, Krishnamurthi S, Rinehart J, Nabell L, Croghan G, Wilner K, *et al.* Clinical aspects of a phase I study of PD-0325901, a selective oral MEK inhibitor, in patients with advanced cancer. *Mol Cancer Ther* 2007; **6**:3649s. (abstract B113). *http://www.sciencedirect.com/science?_ob=ArticleURL&_udi=B6T54-4VKMWBS-4&_user=937415&_coverDate=10%2F08%2F2009&_rdoc=1&_fmt=high&_orig=gateway&_origin=gateway&_sort=d&_docanchor=&view=c&_searchStrId=1694032765&_rerunOrigin=google&_acct=C000048659&_version=1&_urlVersion=0&_userid=937415&md5=d8112eaf600851f6b09b690d5a452dc1&searchtype=a.*

14 Thomson Pharma's HP; *www.thomson-pharma.com.*

15 Adjei AA, Cohen RB, Franklin W, Morris C, Wilson D, Eckhardt SG, *et al.* Phase I pharmacokinetic and pharmacodynamic study of the oral, small-molecule mitogen-activated protein kinase kinase 1/2 inhibitor AZD6244 (ARRY-142886) in patients with advanced cancers. *J Clin Oncol* 2008; **26**:2139–2146. *http://jco.ascopubs.org/content/26/13/2139.abstract?ijkey=86693f9a25dc33babae4808e1f2ca817d9adf20d&keytype2=tf_ipsecsha.*

16 Iverson C, Larson G, Lai C, Yeh LT, Dadson C, Quart B, *et al.* RDEA119/BAY 869766: a potent, selective, allosteric inhibitor of MEK1/2 for the treatment of cancer. *Cancer Res* 2009; **69**:6839–6847. *http://www.ncbi.nlm.nih.gov/pubmed/19706763.*

17 Darzynkiewicz Z, Li X. Measurements of cell death by flow cytometry. In: Cotter TG, Martin SJ, editors. *Techniques in apoptosis: a users' guide.* London: Portland Press. 1996; pp. 71–106.

18 Fischmann TO, Smith CK, Mayhood TW, Myers JE, Reichert P, Madison VS, *et al.* Crystal structures of MEK1 binary and ternary complexes with nucleotides and inhibitors. *Biochemistry* 2009; **48**:2661–2674. *http://pubs.acs.org/doi/abs/10.1021/bi801898e http://www.ncbi.nlm.nih.gov/pubmed/19161339.*

19 Mody N, Leitch J, Armstrong C, Dixon J, Cohen P. Effects of MAP kinase cascade inhibitors on the MKK5/ERK5 pathway. *FEBS Lett* 2001; **502**: 21–24. *http://www.ncbi.nlm.nih.gov/pubmed/11478941.*

20 Daouti S, Wang H, Li WH, Higgins B, Kolinsky K, Niu H, *et al.* Characterization of a novel mitogen-activated protein kinase kinase 1/2 inhibitor with a unique mechanism of action for cancer therapy. *Cancer Res* 2009; **69**:1924–1932. *http://www.ncbi.nlm.nih.gov/pubmed/19244124.*

21 Guo Y, Stacey DW, Hitomi M. Post-transcriptional regulation of cyclin D1 expression during G2 phase. *Oncogene* 2002; **21**:7545–7556. *http://www.nature.com/onc/journal/v21/n49/abs/1205907a.html, http://www.ncbi.nlm.nih.gov/pubmed?term=Oncogene%20(2002)%2021%2C%207545%20%E2%80%93%207556.*

22 Shao J, Sheng H, DuBois RN, Beauchamp RD. Oncogenic ras-mediated cell growth arrest and apoptosis are associated with increased ubiquitin-dependent Cyclin D1. *J Biol Chem* 2000; **275**:22916–22924. *http://www.jbc.org/content/275/30/22916.abstract, http://www.ncbi.nlm.nih.gov/pubmed?term=Oncogenic%20Ras-mediated%20Cell%20Growth%20Arrest%20and%20Apoptosis%20are%20Associated%20with%20Increased%20Ubiquitin-dependent%20Cyclin%20D1.*

23 Dougherty MK, Müller J, Ritt DA, Zhou M, Zhou XZ, Morrison DK, *et al.* Regulation of Raf-1 by direct feedback phosphorylation. *Mol Cell* 2005; **17**:215–224. *http://www.ncbi.nlm.nih.gov/pubmed/15664191.*

24 Yao Z, Okabayashi Y, Yutsudo Y, Kitamura T, Ogawa W, Kasuga M. Role of Akt in growth and survival of PANC-1 pancreatic cancer cells. *Pancreas* 2002; **24**:42–46. *http://www.ncbi.nlm.nih.gov/pubmed/11741181.*

25 Takeda A, Osaki M, Adachi K, Honjo S, Ito H. Role of the phosphatidylinositol 3kinase–Akt signal pathway in the proliferation of human pancreatic ductal carcinoma cell lines. *Pancreas* 2004; **28**: 353–358. *http://www.ncbi.nlm.nih.gov/pubmed/15084985.*

26 Perugini RA, McDade TP, Vittimberga FJ Jr, Callery MP. Pancreatic cancer cell proliferation is phosphatidylinositol 3-kinase dependent. *J Surg Res* 2000; **90**:39–44. *http://www.ncbi.nlm.nih.gov/pubmed/10781373.*

Bioorganic & Medicinal Chemistry 20 (2012) 1910–1921

Contents lists available at SciVerse ScienceDirect

Bioorganic & Medicinal Chemistry

journal homepage: www.elsevier.com/locate/bmc

Target identification of bioactive compounds

Etsu Tashiro, Masaya Imoto *

Department of Biosciences and Informatics, Faculty of Science and Technology, Keio University, 3-14-1 Hiyoshi, Kohokuku, Yokohama, Kanagawa 223-8522, Japan

ARTICLE INFO

Article history:
Available online 4 November 2011

Keywords:
Target identification
Bioactive compounds
Protein function
Chemical genetics

ABSTRACT

To fully understand the regulation of cellular events, functional analysis of each protein involved in the regulatory systems is required. Among a variety of methods to uncover protein function, chemical genetics is a remarkable approach in which small molecular compounds are used as probes to elucidate protein functions within signaling pathways. However, identifying the target of small molecular bioactive compounds isolated by cell-based assays represents a crucial hurdle that must be overcome before chemical genetic studies can commence. A variety of methods and technologies for identifying target proteins have been reported. This review therefore aims to describe approaches for identifying these molecular targets.

1. Introduction

To improve our understanding of complex cell systems, functional analysis of proteins has become a significant focus for a growing number of research fields in biology in the post-genome era.[1] Proteins play an intrinsic role in the cellular events of cell growth, survival, migration, and differentiation, through the sequential assembly of protein interactions, which form signal transduction pathways. However, the role of proteins in many cellular events remains unknown. Among a variety of methods to uncover protein function, chemical genetics is a remarkable approach in which small molecular compounds are used as probes to elucidate protein functions within signaling pathways.[2,3] Indeed, several bioactive compounds have led to breakthroughs in understanding the functional roles of proteins. For example, the study of chemical genetics using FK506, which was isolated from a microbial origin as a new immunosuppressant,[4] contributed to the identification of the important role of calcineurin in the immune system, by identifying FKBP12 as a target protein of FK506.[5,6] Another example is the discovery of lactacystin, a new microbial metabolite which induces differentiation in neuroblastoma cells,[7] whose target identification drove the wide application of lactacystin as a proteasomal inhibitor in the field of cell biology.[8–10] There are now a growing number of chemical inhibitors of signal transduction pathways, and these examples demonstrate how chemical genetics can lead us towards understanding cellular events at a molecular level. However, one significant hurdle to developing new chemical probes of biological systems is identifying the target protein of bioactive compounds, discovered using cell-based small-molecule screening. Identification of the molecular target of bioactive compounds is the major barrier to advancing chemical genetic research. This review therefore aims to describe approaches for identifying these molecular targets.

A variety of methods and technologies for identifying target proteins have been reported. These can be fundamentally categorized into two approaches: direct and indirect.[11] In the direct approach, proteins bound to each compound are purified and directly identified using time-of-flight mass spectrometry (TOF/MS) analysis. Compounds are immobilized using affinity beads or columns to purify the bound proteins (Fig. 1A and Table 1). In this respect, chemical synthesis of the compounds would become a great help for the preparation of the immobilized compounds. However, in the case of natural products, this synthesis is sometimes difficult because of the chiral centers and unique scaffolds in their structures.

On the other hand, the indirect approach offers target candidates by profiling the biological data of the compounds.[11] In the case that the compound was found to perturb some cellular event whose regulatory signaling pathways had been already reported, by clarifying which step within the pathway was affected by the compound, the enzymatic protein engaged in this step could be raised as the target candidate of the compound. In some cases, '-omics' studies (e.g., proteomics, transcriptomics) can help to collect comprehensive data about the biological effects of particular compounds to aid target profiling (Fig. 1B and Table 1).

2. Direct approach

Traditional approaches using affinity chromatography, biochemical fractionation, and radioactive ligand binding assays have been successful in identifying the biological targets of multiple

* Corresponding author.
E-mail address: imoto@bio.keio.ac.jp (M. Imoto).

0968-0896/$ - see front matter © 2011 Elsevier Ltd. All rights reserved.
doi:10.1016/j.bmc.2011.10.081

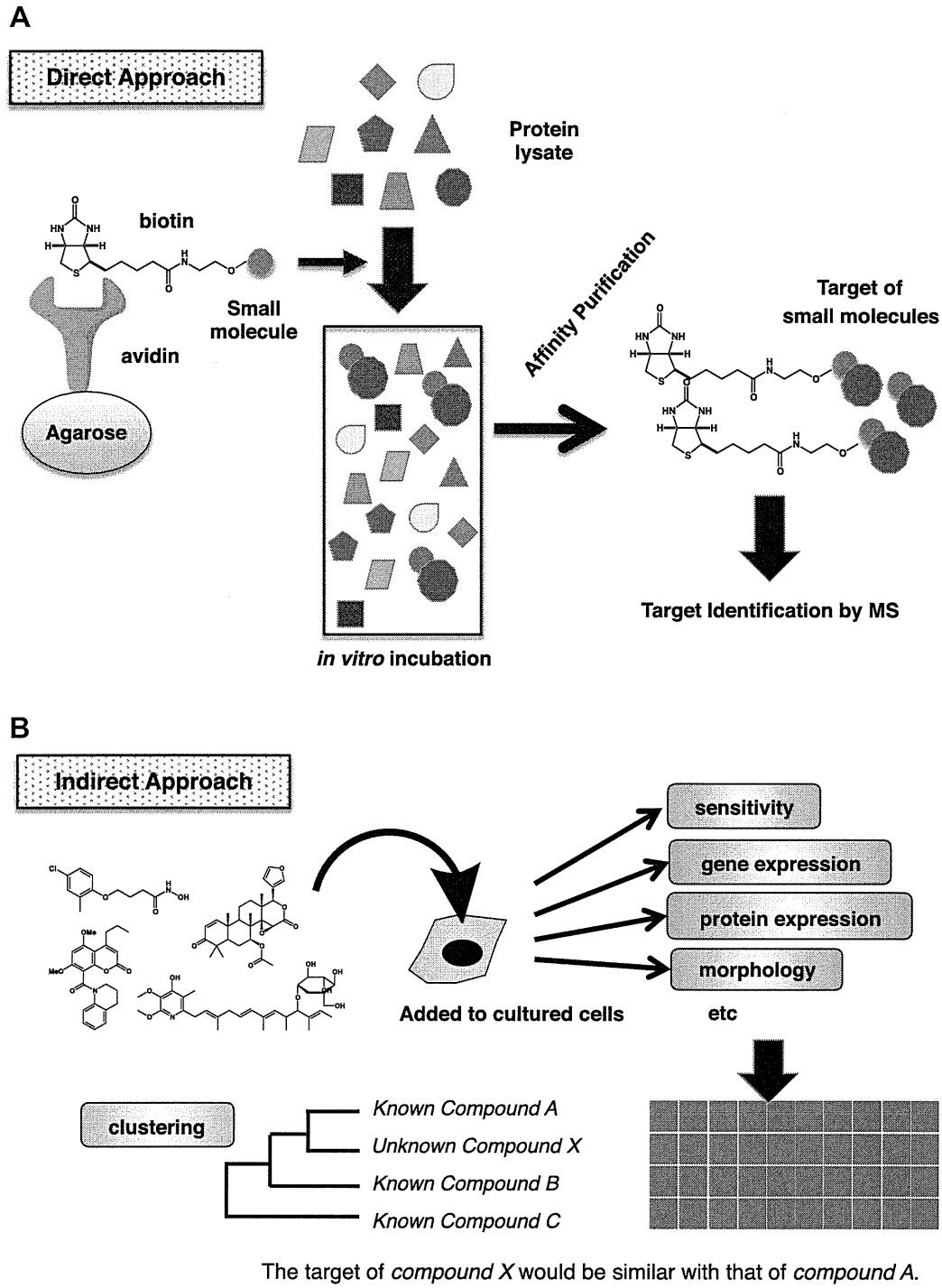

Figure 1. Schematic illustration of 'Direct Approach' and 'Indirect Approach'. (A) The strategy of target identification by using biotin-affinity tags is shown. Cell lysates are incubated with biotin-tagged small molecules and the binding-protein is purified with avidin-agarose before identification using mass spectrometry (MS). (B) The strategy of target identification by profiling is shown. Target-known and target-unknown small molecules are added to cultured cells and the cellular responses, such as drug sensitivity, gene expression, protein expression, or morphological changes, are collected. The profiling from the collected data predicts the target of the small molecule of interest.

small molecules. In particular, affinity chromatography using a biotin affinity tag or Affi-gel system has been successful, but is disadvantaged by the fact that small molecules can lose their biological activity due to the presence of the biotin affinity tag or Affi-gel tag at the active site. To overcome this issue, new methods such as click chemistry, photo-crosslink, and FG beads are now in development. This section highlights recent successes using affinity chromatography as the 'Direct approach'.

2.1. Biotin affinity tag

Target identification using a biotin-affinity tag was first developed by Professor Stuart L. Schreiber.[12] At present, this method was believed to be a powerful tool to identify target proteins. Indeed, many target proteins have since been identified using this method, including target proteins of chromeceptin,[13] withaferin A,[14] tetrahydroisoquinoline,[15] spliceostatin,[16] pladienolide,[17] and

fatostatin[18] (Fig. 2). Chromeceptin was identified as an inhibitor for insulin-induced adipogenesis,[19] and was suggested to exert its biological activity by blocking the autocrine loop of IGF2. Furthermore, chromeceptin activates the transcription factor STAT6, resulting in up-regulation of IGFBP-1 (IGF binding protein 1) and SOCS-3 (suppressor of cytokine signaling 3). IGFBP-1 is known to be a secreted IGF-binding polypeptide which inhibits IGF2. On the other hand, SOCS-3 is reported to suppress insulin-induced tyrosine phosphorylation of insulin receptor substrate (IRS-1), causing insulin resistance. Therefore, chromeceptin was suggested to inhibit insulin-induced adipogenesis through STAT6-stimulated IGFBP-1 and SOCS-3 up-regulation. However, its precise mechanism of action was unknown. Uesugi and co-workers identified MFP-2 (multifunctional protein 2), which is involved in the peroxisomal β-oxidation of fatty acids, as a chromeceptin-binding protein by affinity purification using biotinylated-chromeceptin.[13] Knockdown of MFP-2 suppressed chromeceptin-increased IGFBP-1 expression. These results collectively suggest that MFP-2 is essential for chromeceptin-induced STAT6 activation. Their study provided chemical genetic support for the role of the STAT-SOCS pathway in IGF regulation, and implicated a new pathway for STAT6 activation.

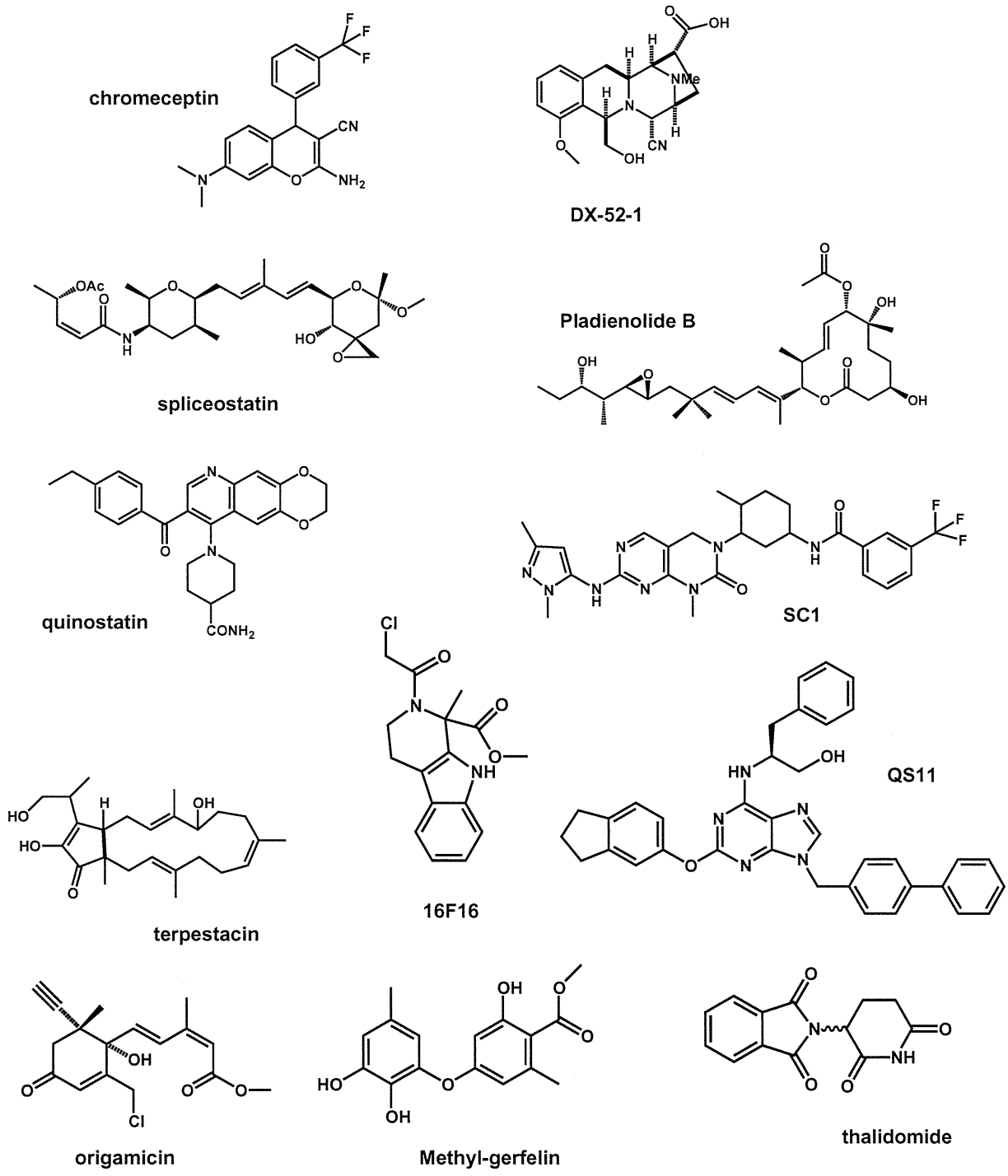

Figure 2. Structure of small molecules whose targets were identified by the 'Direct Approach'.

Table 1
Summary of small molecules whose targets were identified by the 'Direct Approach' or the 'Indirect Approach'

Method category		Compound name	Original bioactivity	Target protein	Journal	First author	Year
Direct approach	Biotin-affinity tag	Chromeceptin	Anti-adipogenesis	MFP-2	Chem. Biol.	Yongmun Choi	2006
		Withaferin A	Anti-cell migration	Annexin-II	Nat. Chem. Biol	Ryan R. Falsey	2006
		DX-52-1	Anti-cell migration	Radixin	Chem. Biol.	Alem W. Kahsai	2006
		DX-52-1	Anti-cell migration	Galectin-3	J. Biol. Chem.	Alem W. Kahsai	2008
		Spliceostatin	Anti-tumor	SF3b	Nat. Chem. Biol.	Daisuke Kaida	2007
		Pladienolide	Anti-tumor	SF3b	Nat. Chem. Biol.	Yoshihiko Kotake	2007
		Fatostatin	Anti-adipogenesis	SCAP	Chem. Biol.	Shinji Kamisuki	2009
	Affi-Gel tag	SC1	Regulation of self-differentiation of ES cells	RasGAP/ERK1	PNAS	Shinji Kamisuki	2009
		Quinostatin	mTOR inhibitor	PI3K p110	Chem. Biol.	Jiong Yang	2007
		QS11	TCF transcriptional activation	ARFGAP1	PNAS	Qisheng Zhang	2007
	Phage display	Terpestacin	Anti-angiogenic	UQCRB (mitochondrial complex III)	J. Biol. Chem.	Hye Jin Jung	2010
	Click chemistry	Origamicin	Anti-HCV activity	PDI	Chem. Biol.	Bojana Rakic	2006
		16F16	Anti-huntingtin	PDI	Nat. Chem. Biol.	Benjamin G. Hoffstrom	2010
	Photo-crosslink	Methyl-gerfelin	Anti-cell migration	Glyoxalase I	PNAS	Makoto Kawatani	2008
	FG-beads	Thalidomide	Teratogenicity	Cereblon	Science	Takumi Ito	2010
Indirect approach	DARTS	Resveratrol	Antioxidant	eIF4A	PNAS	Brett Lomenick	2009
	COMPARE analysis	ZSTK474	Kinase inhibitor	PI3K	J. Netl. Can. Inst.	Shin-ichi Yaguchi	2006
	Connectivity Map	Gedunin	Anti-malarial activity	HSP90	Cancer Cell	Haley Hieronymus	2006
		Celasteol	Growth inhibition	HSP90	Cancer Cell	Haley Hieronymus	2006
		Droxinostat	Enhancing CH-11-induced apoptosis	HDAC	Mol. Cancer Ther.	Tabitha E. Wood	2010
	Proteomic profiling	BNS-22	Growth inhibition	Topoisomerase II	Chem. Biol.	Makoto Kawatani	2011
	Morphological profiling	Pseudolarix acid B	Anti-fungal activity	Microtubule	Nat. Chem. Biol.	Daniel W. Young	2008
		Bisebromoamide	Cytotoxicity	Actin	ACS Chem. Biol.	Eriko Sumiya	2011
		Miuraenamide A	Anti-fungal activity	Actin	ACS Chem. Biol.	Eriko Sumiya	2011
	Metabolomic profiling	Glucopiericidin A	Filopodia inhibition	Glucotransporter	Chem. Biol.	Mitsuhiro Kitagawa	2010
	Chemical-genetic profiling	Papuamide B	Anti-HIV activity	Phosphatidylserine	Cell	Ainslie B. Parsons	2006
		Leucascandrolide	Cell growth inhibition	Cytcrome bc1 complex	Nat. Chem. Biol.	Olesya A. Ulanovskaya	2008
		Theonellamide F	Anti-fungal activity	3β-Hydroxysterols	Nat. Chem. Biol.	Shinichi Nishimura	2010

Tetrahydroisoquinoline DX-52-1, a semi-synthetic derivative of quinocarmycin, was identified as an inhibitor of cell migration.[20] By using biotinylated-DX-52-1, Fenteany and co-workers reported that radixin was the primary target of DX-52-1.[20] Radixin is a member of the ezrin/radixin/moesin (ERM) family of membrane-actin cytoskeleton linker proteins,[21] and ERM family proteins have been reported to bind to actin and various cell adhesion molecules, such as CD44. To elucidate the involvement of radixin in DX-52-1-inhibited cell migration, the authors investigated the effects of DX-52-1 on cell migration in radixin-overexpressing or radixin-knockdown cells. Overexpression of radixin made cells less sensitive to the anti-migratory activity of DX-52-1, whereas radixin knockdown using siRNA resulted in a reduced rate of cell migration, suggesting that radixin plays an important role in DX-52-1-inhibited cell migration. To further address the biological function of radixin in DX-52-1-inhibited cell migration, the authors examined the interaction between radixin and actin or CD44. They found that DX-52-1 disrupted radixin's ability to interact with both actin and CD44, which resulted in an inhibition of cell migration. On the other hand, although radixin was the most intensely labeled protein by biotinylated-DX-52-1, three other less intensely labeled proteins were also detected. Further research aimed at identifying these other proteins found that galectin-3, a family of lectins, was a secondary target of DX-52-1.[15] Similar to radixin, overexpression of galectin-3 decreased sensitivity to the anti-migratory activity of DX-52-1, whereas knockdown of galectin-3 resulted in decreased cell motility and cell adhesion. These results also suggested that galectin-3 plays an important role in DX-52-1-inhibited cell migration. However, the functional correlation between radixin and galectin-3 in cell motility and cell adhesion remains unclear.

The natural product FR901464 was isolated from a fermentation broth of the bacterium *Pseudomonas* sp. as an anti-cancer compound that enhances the transcriptional activity of the SV40 promoter, causes cell cycle arrest at the G1 and G2/M phases,[22,23] and induces abnormal mRNA splicing. However, the molecular mechanism of FR901464 was unknown. Yoshida et al. performed a SAR study to identify which moiety of FR901464 could be attached to biotin, without losing its biological activity. They succeeded in synthesizing a more potent methyl ketal derivative of FR901464, named spliceostatin, and also in synthesizing biotinylated-spliceostatin. By using biotinylated-spliceostatin, they were able to identify the SF3b complex, a subcomplex of the U2 small nuclear ribonucleoprotein (snRNP) in the spliceosome, as a target of spliceostatin. As SF3b has an important role in the U2 snRNP, which binds to the mRNA branchpoint sequence, spliceostatin

was shown to inhibit in vitro and in vivo splicing and promote pre-mRNA (unspliced mRNA) accumulation by binding to SF3b. Furthermore, spliceostatin leaks pre-mRNA into the cytosol, where it is translated. This study showed that the inhibition of pre-mRNA splicing during early steps involving SF3b allows unspliced mRNA leakage and translation.[16] Interestingly, SF3b was also identified as a target of pladienolide by Mizui et al.[17] Pladienolide was isolated from the fermentation broth of *Streptomyces platensis* Mer-11107 as an anti-tumor macrolide, which was discovered by using a cell-based reporter gene expression assay controlled by the human vascular endothelial growth factor promoter.[24–26] They first synthesized fluorescence-tagged pladienolide to monitor the intracellular localization of the target protein. HeLa cells treated with fluorescence-tagged pladienolide showed localization of the pladienolide to the granular structure in the nuclei. These granules overlapped with the localization of splicing factor SF3b. Furthermore, SF3b was confirmed to be a target of pladienolide by purification of the binding protein using biotinylated-pladienolide. Like spliceostatin, pladienolide also inhibited in vivo splicing. These two small molecules showed anti-tumor activity, and these studies suggest that the SF3b complex is a potential anti-tumor drug target. Indeed, pladienolide is now in phase I clinical trials.

2.2. Affi-Gel tag

As well as the biotin affinity tag, purification of the target protein using Affi-gel is also an excellent strategy. The Affi-gel matrix is able to directly link to the small molecule of interest. Thus, compared with the biotin-affinity tag, the number of non-specific interactions with the affinity matrix is reduced. Here, we highlight target proteins of several bioactive small molecules which were identified by using the Affi-gel system. Embryonic stem cells (ES cells) provide an excellent in vitro system for the study of early development and human disease. However, the mechanisms that govern their self-renewal and differentiation are largely unknown. Thus, small molecules that maintain self-renewal or promote differentiation would be useful discoveries to understand self-renewal and differentiation mechanisms. SC1, a derivative of 3,4-dihydropyrimido[4,5-*d*]pyrimidine, was identified to maintain the undifferentiated phenotype of mouse ES (mES) cells by Ding et al.[27] To identify the cellular target of SC1, SC1 was linked at the N1 position to an agarose affinity matrix via a polyethylene glycol linker. Whole-cell lysates of mES cells were incubated with this affinity matrix and the binding proteins were purified and analyzed by liquid chromatography–mass spectrometry (LC/MS). As a result, the SC1-binding proteins were identified as ERK1 and RasGAP. Direct binding of SC1 to ERK1 or RasGAP was confirmed by surface plasmon resonance (SPR). Further biochemical and cellular experiments suggested that SC1 works through dual inhibition of ERK1 and RasGAP.

The mammalian target of the rapamycin (mTOR) signaling network is crucial for the regulation of cell growth in response to both growth factors and nutrients. Although carbon and nitrogen sources, such as glucose and glutamine, are primary stimuli of mTOR, the mechanism by which they stimulate the mTOR pathway are still unknown. Thus, Schreiber and co-workers screened small molecule modulators of mTOR signaling.[28] From a collection of ~20,000 compounds in the library, they discovered quinostatin as an inhibitor of mTOR signaling. Since the molecular target of quinostatin was unknown, they carried out affinity chromatography purification to identify this target protein. An analog of quinostatin was prepared by attaching a polyethylene glycol linker, and this polyethylene glycol-modified quinostatin was immobilized to agarose beads. To isolate the target protein of quinostatin, MCF7 cell lysates were incubated with the affinity reagent. After LC/MS analysis, the target protein of quinostatin was found to be the catalytic subunit of the class Ia PI3Ks.

Similarly, QS11, a purine derivative, that synergizes with a Wnt-3a ligand in the activation of Wnt/β-catenin signal transduction, was shown to bind the GTPase activating protein of ADP-ribosylation factor 1 (ARFGAP1) by using the Affi-Gel system. ARFGAPs form a family of GTPase-activating proteins that regulate the small GTPase ADP-ribosylation factors (ARFs). ARFGAPs promote ARF inactivation by stimulating GTP hydrolysis, whereas guanine nucleotide exchange factors of ARF (ARFGEFs) catalyze the formation of active GTP-bound ARFs. QS11 significantly increased the levels of GTP-bound ARFs in NIH3T3 cells, suggesting that QS11 inhibited ARFGAPs. It has been reported that the activation of ARFs promotes the dissociation of membrane-bound β-catenin.[29] Thus, QS11 was suggested to inhibit ARFGAP, thereby leading to an increase in activated ARF and subsequent β-catenin translocation. The released β-catenin accumulates and translocates to the nucleus when cells are stimulated with Wnt-3a.

2.3. Phage display

Terpestacin was identified to inhibit the functional response to hypoxia of human umbilical vein endothelial cells in vitro and angiogenesis within the embryonic chick chorioallantonic membrane in vivo.[30] Furthermore, terpestacin has been shown to inhibit hypoxia-induced HIF-1α and VEGF expression. These results indicate that terpestacin inhibits hypoxia-induced tumor angiogenesis via the inhibition of HIF-1α-mediated VEGF expression. To better understand the cellular mechanisms of its anti-angiogenic activity, Kwon et al. aimed to identify the target molecule for terpestacin by using phage display biopanning.[31] They first synthesized biotinylated-terpestacin, which was then immobilized on a streptavidin-coated well plate, and four rounds of phage biopanning were conducted using T7 phages expressing functional human cDNA libraries. As a result, UQCRB, a 13.4 kDa subunit of complex III in the mitochondrial respiratory chain,[32] was identified as a terpestacin-binding protein. Knockdown of UQCRB by siRNA resulted in inhibition of hypoxia-induced HIF-1α accumulation and VEGF expression in HT1080 cells. These results suggest that UQCRB plays a key role in the cellular oxygen-sensing and transduction systems. This study provided a new insight into the oxygen-sensing role of UQCRB in mitochondrial complex III.

2.4. Click chemistry

Affinity purification using biotin- or fluorescence-tagged small molecules is a powerful tool for target identification, but biotin- or fluorescence-modifications at the biologically active site of interest can result in a complete loss of activity. To overcome this problem, azide alkyne Huisgen cycloaddition chemistry (a common technique within so-called 'click chemistry') was adapted for target identification. The advantage of using this approach is that minimal structural modification is introduced to the small molecule of interest, without any loss of biological activity. Once the alkyne-derivatized small molecule is covalently bound to its target protein, a tag (e.g., fluorescein-azide or rhodamine-azide) can subsequently be attached via click chemistry.

Click chemistry was first adapted for live cell labeling by Bertozzi et al.[33] Jurkat cells were incubated with Ac_4-ManNAz to introduce SiaNAz residues into their cell-surface glycoproteins. Then, the azide-modified cell-surface glycoproteins were labeled with biotinylated cyclooctyne by using click chemistry. Therefore, the azide-modified cell-surface glycoproteins could be analyzed by flow cytometer with FITC-avidin. This is the first report to employ the reaction for the selective chemical modification of living cells.

Pezacki et al. used click chemistry reactions to identify the target protein of origamicin, an inhibitor of HCV replication.[34] Small molecules that interfere with host-viral interactions are potentially powerful tools for elucidating the molecular mechanisms of pathogenesis and defining new strategies for therapeutic development. Thus, Pezacki et al. screened for HCV replication inhibitors in their established ABA ((+)-S-abscisic acid) library based on the plant hormone ABA, a carotenoid-derived sesquiterpene. As a result, origamicin was identified as an HCV replication inhibitor. Because origamicin has an alkyne moiety in its structure, they exploited it to conjugate both rhodamine for in-gel fluorescence experiments and biotin for affinity chromatography experiments by using click chemistry. The purified protein from using biotinylated-origamicin was identified via LC–MS/MS as protein disulfide isomerase (PDI).

Stockwell et al. screened an inhibitor that suppresses cell death induced by polyglutamine-expanded huntingtin exon 1 (a cell-based model of Huntington's disease) from a 68,887 small-molecule library containing natural products and synthetic small molecules.[35] One hit was small molecule 16F16, and Stockwell et al. synthesized both biotin- and fluorescein-tagged 16F16. However, the modified 16F16 lost its biological activity, so they then used click chemistry. Lysates of PC12 were prepared and incubated with alkyne-derivatized 16F16 to bind to a target protein. Alkyne-derivatized 16F16 was coupled to rhodamine-azide via a click chemistry reaction. Next, fluorescent-tagged target proteins were affinity-purified, analyzed by SDS–PAGE and identified by MS as rat PDI (protein disulfide isomerase) precursors, PDIA1 and PDIA3. Expression of polyglutamine-expanded huntingtin exon 1 in PC12 cells caused PDI to concentrate at ER-mitochondrial junctions and triggered apoptosis via mitochondrial outer-membrane permeabilization. These studies demonstrated a novel strategy for identifying target proteins of small molecules.

2.5. Photo-crosslink

An additional method for overcoming the problem of a loss of biological activity of small molecules due to the presence of an affinity tag is photo-crosslink. Osada et al. developed this new method, which enables the introduction of a variety of small molecules onto solid supports through a photoaffinity reaction.[36] In this method, aryldiazirine groups covalently attached to solid supports are transformed upon UV irradiation into highly reactive carbenes, which are expected to bind to or insert irreversibly into proximal small molecules in a functional-group-independent manner. Osada et al. applied this method to methyl-gerfelin,[37] which had been found to suppress osteoclastogenesis. To understand the molecular mechanism by which this occurred, methyl-gerfelin was immobilized on agarose beads via a photoaffinity linker which they had developed. Binding proteins were purified and analyzed by MALDI-TOF MS, and glyoxalase I (GLO1) was identified as a methyl-gerfelin-binding protein. GLO1 knockdown interfered with osteoclast generation, and methyl-gerfelin competitively inhibited GLO1 enzymatic activity. These results suggest that methyl-gerfelin targets GLO1, resulting in the inhibition of osteoclastogenesis.

2.6. FG beads

Affinity purification using conventional matrices has several disadvantages, including nonspecific binding of irrelevant proteins to the affinity matrices and instability of these matrices. To overcome these issues, Handa and co-workers designed nonporous and physically stable, submicron-sized particles for affinity chromatography. In order to avoid nonspecific protein binding and to allow easy surface modification, they used polymer materials as components of the particles so that their surfaces possessed moderate hydrophilicity and an appropriate functional group. Based on these considerations, they developed high-performance affinity magnetic beads (FG beads)[38] and aimed to identify the target protein of thalidomide by using FG beads. Thalidomide was sold as a sedative in many countries and was often prescribed to pregnant women as a treatment for morning sickness. However, use of thalidomide causes multiple birth defects such as limb, ear, cardiac, and gastrointestinal malformations.[39–41] Despite considerable effort, little is known about the mechanisms underlying these developmental defects caused by thalidomide. Handa et al. identified cereblon (CRBN) as a thalidomide-binding protein by using FG beads.[42] CRBN was originally identified as a candidate gene for autosomal recessive mild mental retardation.[43] Although CRBN was reported to interact with DDB1,[44] which is a component of E3 ubiquitin ligase complexes containing Cullin 4 (Cul4A and Cul4B),[45] the functional relevance of this interaction remained unclear. Based on this information, they demonstrated that CRBN forms an E3 complex with DDB1 and Cul4A. Furthermore, thalidomide inhibited E3 ubiquitin ligase activity of the CRBN-containing complex due to its binding to CRBN. Next, to investigate whether the teratogenic effect of thalidomide could be observed in CRBN-knockdown animals, Handa et al. used zebrafish. CRBN-knockdown zebrafish by use of morpholino oligonucleotides exhibited specific defects in fin and otic vesicle development, which was a similar phenotype to those of thalidomide-treated embryos. Thus, thalidomide was shown to exert its teratogenic effects by binding to CRBN and inhibiting the associated ubiquitin ligase activity.

3. Indirect approach

Affinity chromatography is the most used and most successful method for identifying biological targets of multiple small molecules of interest. However, target identification using affinity chromatography begins with a structure–activity relationship (SAR) study, because we have to know which site(s) are nonessential to use as points of attachment to an affinity tag (e.g., biotin) or solid matrix (e.g., Affi-Gel agarose beads). Therefore, the primary limitation of affinity chromatography is the need to synthesize derivatives of small molecules. SAR studies are time-consuming and require extensive medicinal chemistry expertise. Furthermore, since biologically-active small molecules demonstrate vast structural diversity and complexity, many small molecules cannot be modified without affecting bioactivity, or cannot be easily obtained or synthesized in quantities large enough to permit SAR and subsequent studies. Because of these issues, target identification of small molecules using affinity chromatography is severely limited. This section highlights several 'Indirect Approaches' to overcome the limitations of the previously listed 'Direct Approaches' (Figs. 1B and 3).

3.1. DARTS (drug affinity responsive target stability)

To overcome the limitations of affinity chromatography described above, Huang and co-workers developed DARTS (Fig. 4). The strategy of DARTS is based on the principle that binding of drugs will stabilize target proteins, either globally or locally, for example, in a specific conformation or simply by masking protease recognition sites, thereby reducing the protease sensitivity of the target protein.[46–48] Thus, Huang et al. hypothesized that this could be exploited for target identification without requiring modification or immobilization of the small molecules. As a proof-of-principle, they first demonstrated that DARTS could identify FKBP12 as an FK506-binding protein.[49] Next, they aimed to apply DARTS to identify a molecular target of resveratrol, a small

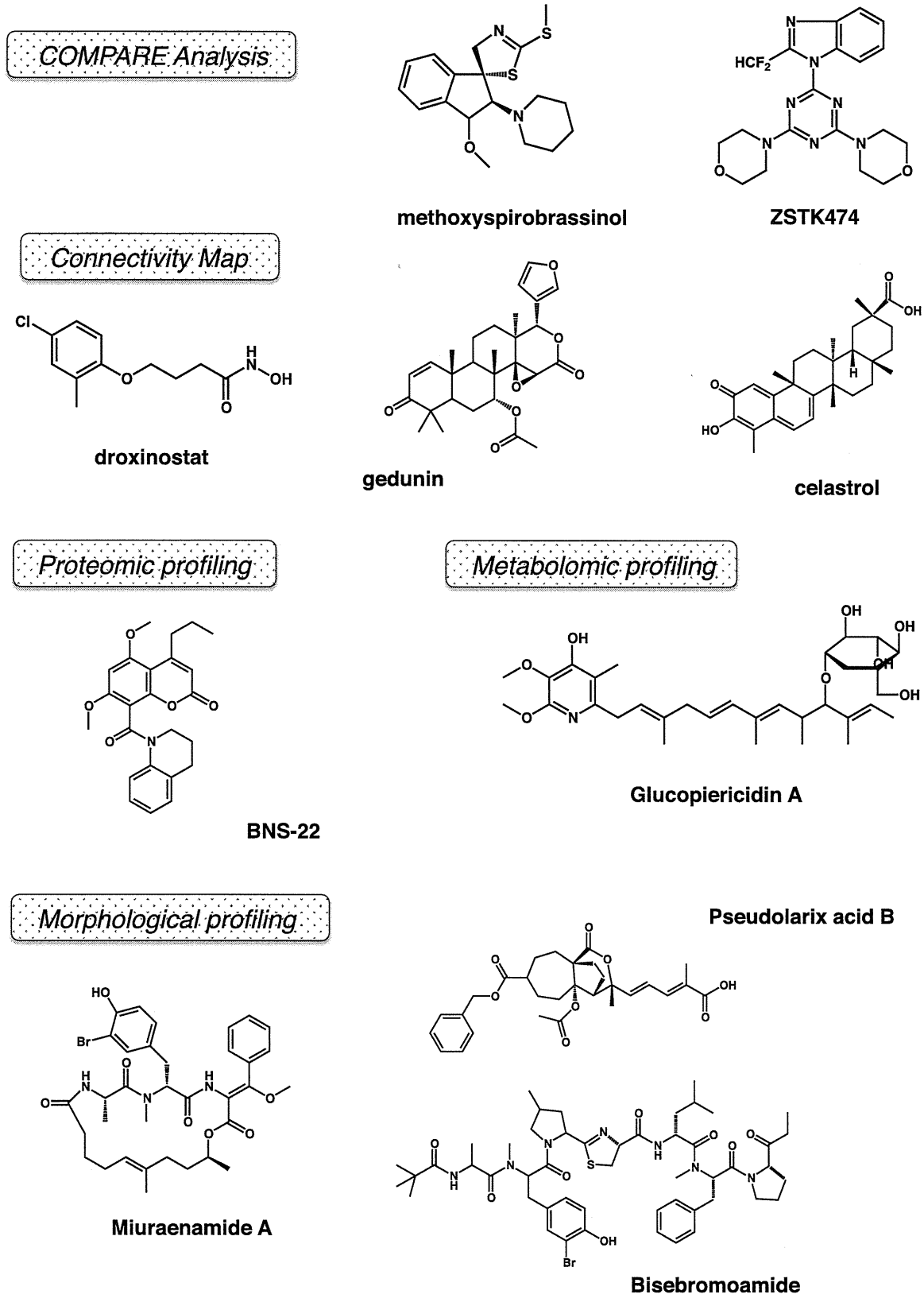

Figure 3. Structure of small molecules whose targets were identified by the 'Indirect Approach'.

molecule in red grapes and wine known for various health benefits including lifespan extension.[50]

Yeast cell lysates or human HeLa cell lysates were treated with resveratrol in vitro, followed by thermolysin digestion and silver staining after separation by SDS–PAGE. Bands of resveratrol-treated lysate protected from thermolysin digestion were analyzed by MS, and were identified as eIF4A (eukaryotic translation initiation factor 4A), a component required for the binding of mRNA to

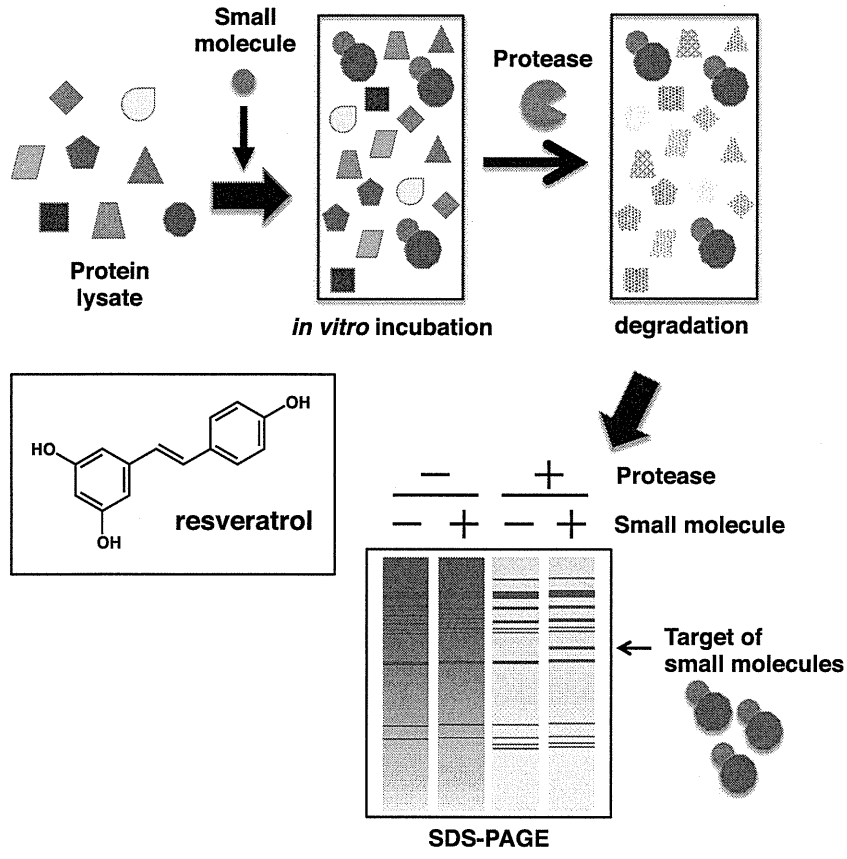

Figure 4. Schematic illustration of DARTS. Yeast or mammalian cultured cell lysates were prepared and treated with small molecules of interest in vitro, followed by protease digestion and silver staining after separation by SDS–PAGE.

40S ribosomal subunits. Purified wild-type eIF4A could be protected by resveratrol from proteolysis, suggesting that resveratrol directly bound to eIF4A. Furthermore, to address whether eIF4A is a target of resveratrol in vivo, they investigated the effect of resveratrol on EMCV IRES-mediated and HCV-mediated translation. Since it has been demonstrated that eIF4A is required for EMCV IRES-mediated translation but not HCV IRES-mediated translation, it follows that resveratrol inhibited EMCV-mediated but not HCV-mediated translation in HEK293 cells. These results indicated that resveratrol inhibited the biological function of eIF4A in vivo. On the other hand, because resveratrol extends lifespan,[50] they asked whether eIF4A is required for resveratrol's longevity effect. Whereas resveratrol lengthens the lifespan of wild-type N2 worms, this longevity effect is lost in eIF4A knockdown worms. These data suggested that eIF4A is a physiological target of resveratrol. Because DARTS does not require labeled small molecules and instead uses 'native' small molecules for binding, it is not limited by chemistry and can potentially be used for any small molecules.

3.2. Profiling

Apart from traditional target identification techniques such as affinity chromatography, new tools have emerged that can significantly aid mechanism elucidation efforts. The development of pattern matching algorithms that compare transcription profiles, drug susceptibility profiles, or morphological profile data, for example, to analogous data on compounds with known cellular targets, allow for mechanistic insights without the need to synthesize chemically-modified probes. Therefore, we next focus on new approaches using these pattern matching and chemical genomic tools.

3.3. COMPARE analysis

The National Cancer Institute established a panel of 60 human cancer cell lines (NCI60) derived from various organs. In a COMPARE analysis, the pattern of toxicity of small molecules to the NCI60 cell line panel is compared. Small molecules that have similar patterns of toxicity are highly correlated in the COMPARE algorithm; such a result suggests the small molecules have a similar mechanism of action, and indeed COMPARE has been successfully used in target identification studies. For example, 2-piperidyl analogues of natural indole phytoalexins, 1-methoxyspirobrassinols, and *N*-((1-benzyl-1*H*-1,2,3-trizol-4-yl)methyl)arylamide were reported to decrease intracellular glutathione levels[51] and inhibit tubulin polymerization,[52] respectively. Phytoalexins are small molecules naturally produced by plants. Various indole phytoalexins have been shown to exhibit anti-tumor activities. However, the anti-proliferative activity of most indole phytoalexins had been limited to certain cancer cells, and their mode of action has not been elucidated. Therefore, in order to achieve higher potency, new derivatives of indole phytoalexins have been synthesized. McDonald et al. synthesized 2-piperidyl analogues of indole phytoalexins, *cis*-1-Boc-, *trans*-1-Boc-, *cis*-1-methoxy- and *trans*-1-methoxy-2-deoxy-2-(1-piperidyl)spirobrassinols, and these derivatives exhibited a more favorable growth-inhibitory effect on some cancer cells than their parent compounds. Furthermore, to elucidate their mode of action, McDonald et al. performed COMPARE analysis with the NCI60 cell line panel. As a result, the profiles of their synthesized indole phytoalexins showed similar patterns with small molecules that deplete intracellular glutathione level, such as *N*-methylformamide and L-buthionine sulfoximine (BSO). Indeed, their synthesized indole phytoalexins decreased intracellular glutathione levels in

MCF-7 cells. Since glutathione is often involved in the resistance of cancer cells to radio- and chemotherapy, these small molecules with remarkable glutathione-depleting potency may be developed as radio- or chemo-sensitizing agents. A series of *N*-((1-benzyl-1*H*-1,2,3-trizol-4-yl)methyl)arylamides are synthetic derivatives of mycobactin S, a natural product produced by *Mycobacterium smegmatis* that exhibits anti-tuberculosis activity.[53] Moller et al. found that their synthesized derivatives showed anti-proliferative effects against human cancer cell lines. To evaluate the mode of action of *N*-((1-benzyl-1*H*-1,2,3-trizol-4-yl)methyl)arylamides, they performed COMPARE analysis with the NCI60 cell line panel. COMPARE analysis revealed that *N*-((1-benzyl-1*H*-1,2,3-trizol-4-yl)methyl)arylamides correlated with paclitaxel, vinblastine, and rhizoxin, all of which affect microtubule polymerization. Although further studies confirmed that *N*-((1-benzyl-1*H*-1,2,3-trizol-4-yl)methyl)arylamides inhibited microtubule polymerization in vitro and in vivo and induced G2/M cell cycle arrest, the mechanism by which *N*-((1-benzyl-1*H*-1,2,3-trizol-4-yl)methyl)arylamides inhibit microtubule polymerization still remains unclear.

Similar to the NCI60 cell line panel, Yamori et al. established a panel of 39 human cancer cell lines (termed JFCR39) coupled to a drug activity database. By using the JFCR39 database, they found that ZSTK474 exhibited similar responses to the PI3K inhibitor LY294002, suggesting that ZSTK474 is a new PI3K inhibitor.[54] Indeed, ZSTK474 was found to directly inhibit PI3K activity more efficiently than the PI3K inhibitor LY294002. Molecular modeling of the PI3K-ZSTK474 complex indicated that ZSTK474 could bind to the ATP-binding pocket of PI3K. These studies strongly suggest that this approach can be used to predict the molecular target or the mode of action of small molecules.

3.4. Connectivity Map database

Whole-genome transcript profiling has emerged as powerful tool to investigate the effects of small molecules on cells. The Connectivity Map database, developed at the Broad Institute, is a publicly accessible database comprised of gene expression data of cells treated with small molecules.[55] The transcript profile data of a compound of interest is compared to analogous data that has been collected on hundreds of small molecules with known molecular targets. The Connectivity Map database has been utilized in mode-of-action studies of several small molecules. For example, droxinostat was first identified as sensitizing malignant cells to the CH-11 Fas-activating antibody.[56] However, the Connectivity Map database revealed that the transcript profile of droxinostat showed a similar response to that of the HDAC inhibitors vorinostat and trichostatin A. Further cell-based and in vitro assays showed that droxinostat is a novel HDAC inhibitor that is selective for HDAC3, HDAC6, and HDAC8 through its hydroxamic acid moiety. To further explore the effects of HDAC inhibitions on Fas sensitization, Schimmer et al. knocked down HDACs with shRNA. As a result, HDAC8 knockdown enhanced sensitivity to Fas. Furthermore, droxinostat or HDAC8 knockdown was shown to decrease FLIP mRNA, a caspase-8 inhibitory protein. These results suggested that droxinostat decreased FLIP via HDAC inhibition, which resulted in sensitization to Fas-induced apoptosis. However, it is unclear whether HDACs inhibition by droxinostat would directly or indirectly decrease FLIP expression. Other examples include gedumin and celastrol. These two small molecules were identified as inhibitors of androgen receptor (AR)-activated signaling in prostate cancer by a high-throughput cell-based screening.[57] The Connectivity Map database revealed that these compounds were predicted to have a similar mode of action to the heat shock protein 90 (HSP90) inhibitors geldanamycin, 17-dimethylamino-geldanamycin and 17-allylaminogeldanamycin. It has been reported that the androgen receptor is a client of HSP90, and HSP90 inhibitors induced AR degradation. Thus, gedunin and celasteol were predicted to inhibit AR signaling by inhibiting HSP90. Indeed, these two compounds induced the down-regulation of AR and several other HSP90 client proteins. Furthermore, these two small molecules inhibited ATP binding to HSP90. However, since gedunin and celasteol did not compete for the ATP-binding site, gedunin and celasteol seem to have distinct mechanisms from geldanamycin. These studies suggested that the Connectivity Map database could also be used to predict the molecular target or the mode of action of small molecules.

3.5. Proteomic profiling

Compared with gene expression profiling like the Connectivity Map database which can simultaneously measure the expression of more than 20,000 genes, proteome analysis provides us with only ~1000 protein spots. However, two-dimensional gel electrophoresis (2DE) analyses often show us any change in molecular weight or isoelectric point of proteins after posttranslational modification as a clear mobility shift of protein spots. Because biologically active small molecules affect cellular processes and induce changes in both the expression level and modification of proteins, proteome profiling is an informative approach for investigating the effects of a small molecule. Osada and co-workers developed a new proteomic profiling system to predict the target protein of small molecules of interest.[58] To compare the proteomic pattern with small molecules whose targets are known, HeLa cells treated with each small molecule were analyzed by 2D-DIGE, and hierarchical clustering was performed. For example, radicicol and geldanamycin (structurally different HSP90 inhibitors), showed a similar proteome pattern, suggesting that this proteomic profiling system discriminates small molecules by mechanism of action. Indeed, the proteomic profiling analysis of BNS-22, a chemically synthesized derivative of the natural plant product GUT-70, showed that BNS-22 belongs to the same cluster as ICRF-193, a DNA topoisomerase II (TOP2) catalytic inhibitor. Further biochemical studies confirmed that BNS-22 targets and acts as a catalytic inhibitor of TOP2.[59]

3.6. Morphological profiling

A recent and rapidly developing technology is high content screening (HCS) that combines automated microscopy with image analysis, enabling phenotypic profiling of small molecules based on the activity of cells visualized by fluorescence cytology. Feng et al. introduced factor analysis as a data-driven tool for defining cell phenotypes and profiling small molecule activity.[60] They used a high-content image assay to screen and profile a library of 6547 small molecules derived from a diversity library (21%), a natural products library (58%) and a library of known bioactive small molecules (21%); all small molecules were assayed in HeLa cells to monitor cell proliferation, and to profile their cell cycle phenotype, using fluorescent probes for DNA (Hoechst 33342 dye), mitosis (anti-phosphoH3) and DNA replication (EdU; 5-ethyl-2-deoxyuridine). Images were automatically acquired and at least 500 cells were scored per treatment. They found that six factors (nuclear size, DNA replication, chromosome condensation, nuclear morphology, EdU texture, and nuclear shape) are sufficient to describe the biological responses. Profiling the small molecule library using these six factors resulted in the clustering of hits into seven phenotypic categories. Feng et al. then compared the phenotypic profiles, chemical similarity and predicted protein-binding activity of these small molecules. For instance, within the subcluster from the mitotic arrest phenotype, which is primarily characterized by high chromosome condensation, the authors observed four distinct

groups of structurally related small molecules; colchicine derivatives, a set of novel kinase inhibitors, quinolone derivatives and a pseudolarix acid B derivative. All of these small molecules have been reported to affect microtubules polymerization.[61–63] Indeed, they demonstrated depolymerization of microtubules and mitotic arrest in cells treated with each of the colchicine, quinolone and pseudolarix acid B derivatives.

Further cell morphological profiling has revealed bisebromoamide and miuraenamide A as actin filament stabilizers. Uesugi et al. used automated high-content image analysis to evaluate the morphology of cells exhibiting nuclear protrusion.[64] Actin-targeting small molecules decreased cytoplasmic area up to ~70%, and increased the distance between the centroid of the nucleus and the centroid of the entire cell. When those two parameters were plotted against each other, points for the seven known actin-targeting small molecules, cytochalasin D,[65] doliculide,[66] jasplakinolide,[67] latrunculin A,[68] mycalolide B,[69] seragamide A,[70] and swinholide A,[71] were clustered together. Based on this morphological profiling, the target of bisebromoamide and miuraenamide A, marine natural products whose targets were previously unknown,[72–75] were predicted to be actin stabilization. Indeed, they showed that bisebromoamide and miuraenamide A stabilized actin filaments in vitro, and fluorescein-conjugated bisebromoamide localized specifically to actin filaments in cells.

3.7. Metabolomics profiling

Metabolomic technologies have advanced tremendously in recent years, and capillary electrophoresis time-of-flight mass spectrometry (CE-TOFMS) has emerged as a powerful new tool for the comprehensive analysis of cellular metabolites.[76,77] The use of CE-TOFMS to understand global metabolism at the system level has become widespread.[78–81] Analysis of the metabolome with CE-TOFMS also reveals metabolic changes induced by small molecules. Thus, despite a lack of reports describing the identification of chemical inhibitor targets using metabolomic analysis, such efforts would be worthwhile. We screened bioactive compounds that inhibit cellular filopodia protrusion in carcinoma. Filopodia

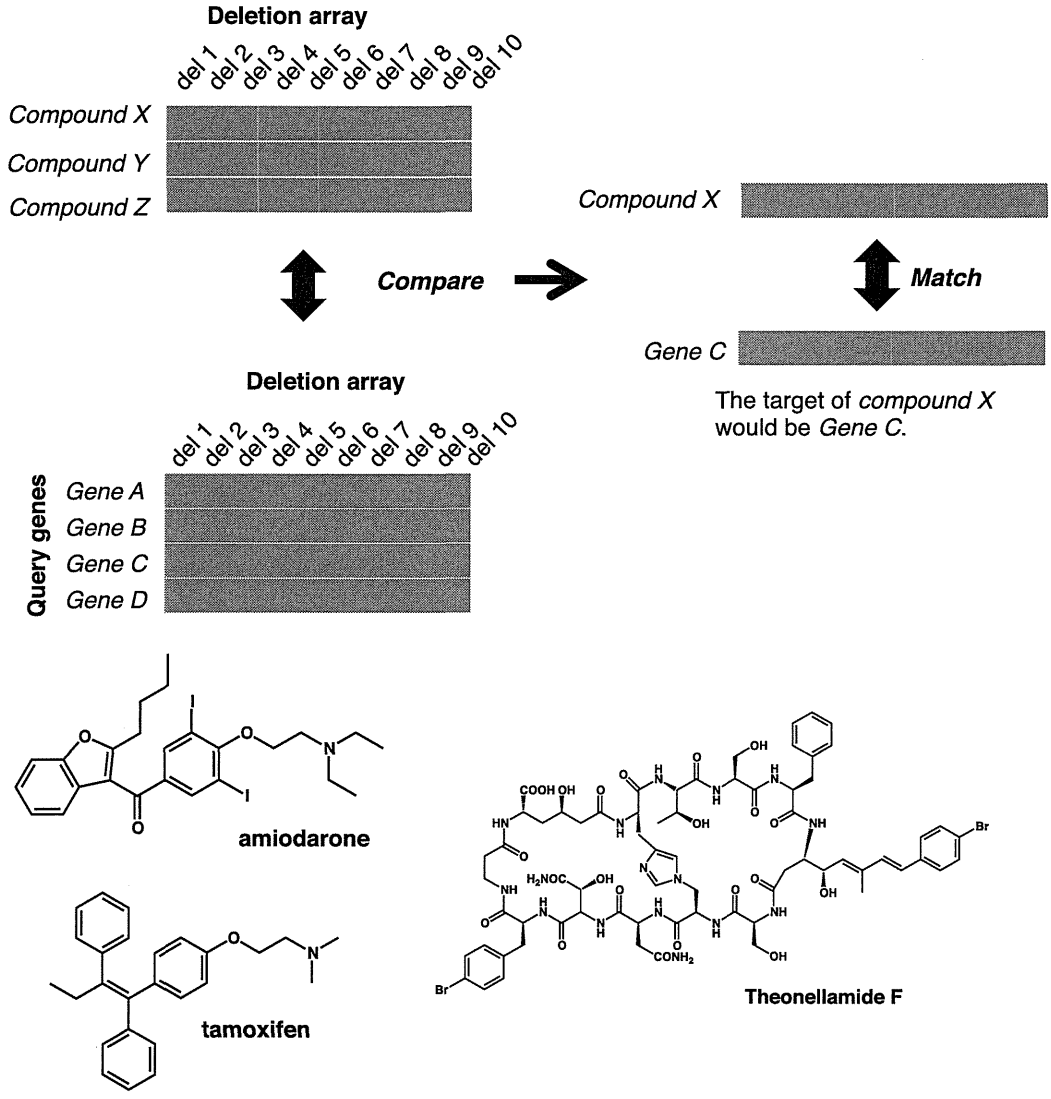

Figure 5. Comparison of a chemical-genetic profile to a compendium of genetic interaction (synthetic lethal) profiles could identify pathways and target genes of small molecules. Conceptually, the comparison of a chemical-genetic profile to the genetic interaction (synthetic lethal) profiles should identify the pathways and targets inhibited by small molecule treatment. For example, deletion mutants del2, del5, del6 and del8 are hypersensitive to compound X and a mutation in query *gene* C leads to a fitness defect when combined with deletion alleles del2, del5, del6 and del8. Here, the chemical-genetic profile of compound X resembles the genetic profile of *gene* C, thereby identifying the product of *gene* C as a putative target of compound X.

are spike-like cell membrane projections contributing to tumor metastasis; however, the molecular mechanisms controlling filopodia protrusion are complicated and unclear.[82,83] Thus, the discovery of a filopodia inhibitor and its molecular target which could be employed in chemical genetic studies may lead to a fuller understanding of filopodia, contributing to the treatment of tumor metastasis. In the course of screening filopodia protrusions from microbial origin, glucopiericidin A was isolated. Biochemical studies raised the possibility that glucopiericidin A would be an inhibitor of glycolysis. To address whether glucopiericidin A actually perturbs glycolysis, the effect of glucopiericidin A on global metabolism and on glycolysis was assessed by measuring the metabolome using CE-TOFMS. CE-TOFMS provided strong evidence that glucopiericidin A suppresses glycolysis by functionally targeting the glucose transporter. Our results represent a success of molecular target identification using metabolomics analysis.[84]

3.8. Chemical-genetic profiling in yeast

In yeast *Saccharomyces cerevisiae*, ~6000 potential genes have been characterized by the genome sequencing project. As each gene has been deleted, ~1000 essential genes and ~5000 viable deletion mutants were identified. Boone et al. generated a compendium of 'chemical-genetic interaction' profiles from scoring ~5000 viable yeast haploid deletion mutant strains for hypersensitivity to a diverse set of small molecules.[85] In addition, they also generated 'genetic interaction (synthetic lethal)' profiles by testing viabilities in each double gene-mutant combination. Conceptually, the comparison of a chemical-genetic profile to the genetic interaction (synthetic lethal) profile should identify the pathways and targets inhibited by small molecule treatment (Fig. 5).

Boone et al. generated chemical-genetic profiles for 82 different conditions by testing the collection of viable yeast haploid deletion mutants for hypersensitivity to 82 small molecules, including 75 synthetic and natural products and 7 crude antifungal extracts derived from different marine sponges and microorganisms.[86] The set of chemical-genetic profiles, visualized by two-dimensional hierarchical clustering, revealed that small molecules with similar cellular effects showed similar chemical-genetic profiles. Examples include (i) actin binding agents latrunculin B[87] and cytochalasin A;[88] (ii) cell wall synthesis inhibitors staurosporine, which targets protein kinase C, a regulator of a MAP kinase cascade involved in cell wall metabolism,[89] and caspofungin, which inhibits 1,3 β-glucan synthase;[90] (iii) radicicol and geldanamycin—although structurally unrelated, both act as highly selective inhibitors of Hsp90 function through their ability to bind within the ADP/ATP binding pocket of the chaperone.[91] Interestingly, the chemical-genetic interactions of amiodarone, an antifungal and anti-arrhythmic small molecule, clusters with tamoxifen, a competitive inhibitor of estradiol binding to the estrogen receptor and a common breast cancer drug. This is notable, as the antifungal activity of amiodarone is the perturbation of calcium homeostasis,[92] and tamoxifen seems to produce an increase in cytosolic Ca^{2+} in yeast. Indeed, both amiodarone and tamoxifen triggered the reporter activity driven by calcineurin-dependent response element (CDRE), suggesting that tamoxifen is a potent activator of calcineurin signaling. Furthermore, two natural product extracts (prior to purification of the active component) that were derived from different organisms and diverse locations, from a sea cucumber from the Commonwealth of Dominica and an Indonesian marine sponge, showed highly similar chemical-genetic profiles. After purification, the active components were identical to stichloroside[93] and theopalauamide,[94] respectively. Both of the purified small molecules display chemical-genetic profiles resembling those of their crude extracts, suggesting that chemical-genetic profiling is an effective means for functional classification of natural product extracts. Taken together, Boone et al. demonstrated the potential for integration of chemical-genetic profiles and genetic interaction profiles to provide information about the pathways and targets affected by bioactive small molecules.

Another example was reported by Yoshida et al.[95] Theonellamides are members of a unique family of bicyclic dodecapeptides isolated from a marine sponge, *Theonella* sp. These small molecules show broad antifungal activity as well as moderate cytotoxicity in mammalian cells.[96,97] Despite screens for binding proteins using theonellamide A affinity beads, their target molecules remain unknown.[98] Therefore, to evaluate the mode of action of theonellamide, Yoshida et al. generated a chemical-genomic profile of theonellamide F, bicyclic peptides derived from a marine sponge, using a collection of fission yeast strains in which each open reading frame (ORF) is expressed under the control of an inducible promoter (fission yeast ORFeome overexpression strain collection).[99,100] The overexpression strains were exposed individually to theonellamide F and a compendium of 10 reference small molecules with known targets at various concentrations. Strains showing a significantly altered sensitivity compared to the control strain were selected. Cluster analysis of the Gene Ontology (GO) terms associated with the genes that alter small molecule sensitivity suggested a mechanistic link between theonellamide and 1,3-β-D-glucan synthesis. Overproduction of 1,3-β-D-glucan was induced by theonellamide F in a Rho1-dependent manner. Furthermore, by using a fluorescent theonellamide derivative, theonellamides were shown to specifically bind in vitro to 3β-hydroxysterols, including ergosterol, and cause membrane damage. Taken together, these results show that theonellamides are a new class of sterol-binding molecules that induce membrane damage and activate Rho1-mediated 1,3-β-D-glucan synthesis.

Acknowledgements

We are grateful to Ms. Yukiko Sasazawa, Ms. Satoko Shinjo, Mr. Kohta Yamamoto, Mr. Shigeyuki Magi, and Mr. Takahiro Fujimaki for supporting some of our work.

References and notes

1. Pandey, A.; Mann, M. *Nature* **2000**, *405*, 837.
2. Alaimo, P. J.; Shogren-Knaak, M. A.; Shokat, K. M. *Curr. Opin. Chem. Biol.* **2001**, *5*, 360.
3. Zheng, X. F.; Chan, T. F. *Drug Discovery Today* **2002**, *7*, 197.
4. Kino, T.; Hatanaka, H.; Hashimoto, M.; Nishiyama, M.; Goto, T.; Okuhara, M.; Kohsaka, M.; Aoki, H.; Imanaka, H. *J. Antibiot. (Tokyo)* **1987**, *40*, 1249.
5. Siekierka, J. J.; Hung, S. H.; Poe, M.; Lin, C. S.; Sigal, N. H. *Nature* **1989**, *341*, 755.
6. Liu, J.; Farmer, J. D., Jr.; Lane, W. S.; Friedman, J.; Weissman, I.; Schreiber, S. L. *Cell* **1991**, *66*, 807.
7. Omura, S.; Fujimoto, T.; Otoguro, K.; Matsuzaki, K.; Moriguchi, R.; Tanaka, H.; Sasaki, Y. *J. Antibiot. (Tokyo)* **1991**, *44*, 113.
8. Fenteany, G.; Standaert, R. F.; Lane, W. S.; Choi, S.; Corey, E. J.; Schreiber, S. L. *Science* **1995**, *268*, 726.
9. Jensen, T. J.; Loo, M. A.; Pind, S.; Williams, D. B.; Goldberg, A. L.; Riordan, J. R. *Cell* **1995**, *83*, 129.
10. Lee, D. H.; Goldberg, A. L. *Trends Cell Biol.* **1998**, *8*, 397.
11. Hart, C. P. *Drug Discovery Today* **2005**, *10*, 513.
12. Galat, A.; Lane, W. S.; Standaert, R. F.; Schreiber, S. L. *Biochemistry* **1992**, *31*, 2427.
13. Choi, Y.; Shimogawa, H.; Murakami, K.; Ramdas, L.; Zhang, W.; Qin, J.; Uesugi, M. *Chem. Biol.* **2006**, *13*, 241.
14. Falsey, R. R.; Marron, M. T.; Gunaherath, G. M.; Shirahatti, N.; Mahadevan, D.; Gunatilaka, A. A.; Whitesell, L. *Nat. Chem. Biol.* **2006**, *2*, 33.
15. Kahsai, A. W.; Cui, J.; Kaniskan, H. U.; Garner, P. P.; Fenteany, G. *J. Biol. Chem.* **2008**, *283*, 24534.
16. Kaida, D.; Motoyoshi, H.; Tashiro, E.; Nojima, T.; Hagiwara, M.; Ishigami, K.; Watanabe, H.; Kitahara, T.; Yoshida, T.; Nakajima, H., et al *Nat. Chem. Biol.* **2007**, *3*, 576.
17. Kotake, Y.; Sagane, K.; Owa, T.; Mimori-Kiyosue, Y.; Shimizu, H.; Uesugi, M.; Ishihama, Y.; Iwata, M.; Mizui, Y. *Nat. Chem. Biol.* **2007**, *3*, 570.
18. Kamisuki, S.; Mao, Q.; Abu-Elheiga, L.; Gu, Z.; Kugimiya, A.; Kwon, Y.; Shinohara, T.; Kawazoe, Y.; Sato, S.; Asakura, K., et al *Chem. Biol.* **2009**, *16*, 882.

19. Choi, Y.; Kawazoe, Y.; Murakami, K.; Misawa, H.; Uesugi, M. *J. Biol. Chem.* **2003**, *278*, 7320.
20. Kahsai, A. W.; Zhu, S.; Wardrop, D. J.; Lane, W. S.; Fenteany, G. *Chem. Biol.* **2006**, *13*, 973.
21. Tsukita, S.; Hieda, Y. *J. Cell Biol.* **1989**, *108*, 2369.
22. Nakajima, H.; Sato, B.; Fujita, T.; Takase, S.; Terano, H.; Okuhara, M. *J. Antibiot. (Tokyo)* **1996**, *49*, 1196.
23. Nakajima, H.; Hori, Y.; Terano, H.; Okuhara, M.; Manda, T.; Matsumoto, S.; Shimomura, K. *J. Antibiot. (Tokyo)* **1996**, *49*, 1204.
24. Mizui, Y.; Sakai, T.; Iwata, M.; Uenaka, T.; Okamoto, K.; Shimizu, H.; Yamori, T.; Yoshimatsu, K.; Asada, M. *J. Antibiot. (Tokyo)* **2004**, *57*, 188.
25. Sakai, T.; Sameshima, T.; Matsufuji, M.; Kawamura, N.; Dobashi, K.; Mizui, Y. *J. Antibiot. (Tokyo)* **2004**, *57*, 173.
26. Sakai, T.; Asai, N.; Okuda, A.; Kawamura, N.; Mizui, Y. *J. Antibiot. (Tokyo)* **2004**, *57*, 180.
27. Chen, S.; Do, J. T.; Zhang, Q.; Yao, S.; Yan, F.; Peters, E. C.; Scholer, H. R.; Schultz, P. G.; Ding, S. *Proc. Natl. Acad. Sci. U.S.A.* **2006**, *103*, 17266.
28. Yang, J.; Shamji, A.; Matchacheep, S.; Schreiber, S. L. *Chem. Biol.* **2007**, *14*, 371.
29. Palacios, F.; Schweitzer, J. K.; Boshans, R. L.; D'Souza-Schorey, C. *Nat. Cell Biol.* **2002**, *4*, 929.
30. Jung, H. J.; Lee, H. B.; Kim, C. J.; Rho, J. R.; Shin, J.; Kwon, H. J. *J. Antibiot. (Tokyo)* **2003**, *56*, 492.
31. Jung, H. J.; Shim, J. S.; Lee, J.; Song, Y. M.; Park, K. C.; Choi, S. H.; Kim, N. D.; Yoon, J. H.; Mungai, P. T.; Schumacker, P. T., et al *J. Biol. Chem.* **2010**, *285*, 11584.
32. Suzuki, H.; Hosokawa, Y.; Toda, H.; Nishikimi, M.; Ozawa, T. *Biochem. Biophys. Res. Commun.* **1988**, *156*, 987.
33. Agard, N. J.; Prescher, J. A.; Bertozzi, C. R. *J. Am. Chem. Soc.* **2004**, *126*, 15046.
34. Rakic, B.; Clarke, J.; Tremblay, T. L.; Taylor, J.; Schreiber, K.; Nelson, K. M.; Abrams, S. R.; Pezacki, J. P. *Chem. Biol.* **2006**, *13*, 1051.
35. Hoffstrom, B. G.; Kaplan, A.; Letso, R.; Schmid, R. S.; Turmel, G. J.; Lo, D. C.; Stockwell, B. R. *Nat. Chem. Biol.* **2010**, *6*, 900.
36. Kanoh, N.; Kumashiro, S.; Simizu, S.; Kondoh, Y.; Hatakeyama, S.; Tashiro, H.; Osada, H. *Angew. Chem., Int. Ed.* **2003**, *42*, 5584.
37. Kawatani, M.; Okumura, H.; Honda, K.; Kanoh, N.; Muroi, M.; Dohmae, N.; Takami, M.; Kitagawa, M.; Futamura, Y.; Imoto, M., et al *Proc. Natl. Acad. Sci. U.S.A.* **2008**, *105*, 11691.
38. Sakamoto, S.; Kabe, Y.; Hatakeyama, M.; Yamaguchi, Y.; Handa, H. *Chem. Rec.* **2009**, *9*, 66.
39. Miller, M. T.; Stromland, K. *Teratology* **1999**, *60*, 306.
40. Melchert, M.; List, A. *Int. J. Biochem. Cell Biol.* **2007**, *39*, 1489.
41. Knobloch, J.; Ruther, U. *Cell Cycle* **2008**, *7*, 1121.
42. Ito, T.; Ando, H.; Suzuki, T.; Ogura, T.; Hotta, K.; Imamura, Y.; Yamaguchi, Y.; Handa, H. *Science* **2010**, *327*, 1345.
43. Higgins, J. J.; Pucilowska, J.; Lombardi, R. Q.; Rooney, J. P. *Neurology* **2004**, *63*, 1927.
44. Angers, S.; Li, T.; Yi, X.; MacCoss, M. J.; Moon, R. T.; Zheng, N. *Nature* **2006**, *443*, 590.
45. Groisman, R.; Polanowska, J.; Kuraoka, I.; Sawada, J.; Saijo, M.; Drapkin, R.; Kisselev, A. F.; Tanaka, K.; Nakatani, Y. *Cell* **2003**, *113*, 357.
46. Park, C.; Marqusee, S. *Nat. Methods* **2005**, *2*, 207.
47. Stankunas, K.; Bayle, J. H.; Gestwicki, J. E.; Lin, Y. M.; Wandless, T. J.; Crabtree, G. R. *Mol. Cell* **2003**, *12*, 1615.
48. Tucker, C. L.; Fields, S. *Nat. Biotechnol.* **2001**, *19*, 1042.
49. Lomenick, B.; Hao, R.; Jonai, N.; Chin, R. M.; Aghajan, M.; Warburton, S.; Wang, J.; Wu, R. P.; Gomez, F.; Loo, J. A., et al *Proc. Natl. Acad. Sci. U.S.A.* **2009**, *106*, 21984.
50. Wood, J. G.; Rogina, B.; Lavu, S.; Howitz, K.; Helfand, S. L.; Tatar, M.; Sinclair, D. *Nature* **2004**, *430*, 686.
51. Mezencev, R.; Kutschy, P.; Salayova, A.; Curillova, Z.; Mojzis, J.; Pilatova, M.; McDonald, J. *Chemotherapy* **2008**, *54*, 372.
52. Stefely, J. A.; Palchaudhuri, R.; Miller, P. A.; Peterson, R. J.; Moraski, G. C.; Hergenrother, P. J.; Miller, M. J. *J. Med. Chem.* **2010**, *53*, 3389.
53. Maurer, P. J.; Miller, M. J. *J. Am. Chem. Soc.* **1983**, *105*, 240.
54. Yaguchi, S.; Fukui, Y.; Koshimizu, I.; Yoshimi, H.; Matsuno, T.; Gouda, H.; Hirono, S.; Yamazaki, K.; Yamori, T. *J. Natl. Cancer Inst.* **2006**, *98*, 545.
55. Lamb, J.; Crawford, E. D.; Peck, D.; Modell, J. W.; Blat, I. C.; Wrobel, M. J.; Lerner, J.; Brunet, J. P.; Subramanian, A.; Ross, K. N., et al *Science* **2006**, *313*, 1929.
56. Wood, T. E.; Dalili, S.; Simpson, C. D.; Sukhai, M. A.; Hurren, R.; Anyiwe, K.; Mao, X.; Suarez Saiz, F.; Gronda, M.; Eberhard, Y., et al *Mol. Cancer Ther.* **2010**, *9*, 246.
57. Hieronymus, H.; Lamb, J.; Ross, K. N.; Peng, X. P.; Clement, C.; Rodina, A.; Nieto, M.; Du, J.; Stegmaier, K.; Raj, S. M., et al *Cancer Cell* **2006**, *10*, 321.
58. Muroi, M.; Kazami, S.; Noda, K.; Kondo, H.; Takayama, H.; Kawatani, M.; Usui, T.; Osada, H. *Chem. Biol.* **2010**, *17*, 460.
59. Kawatani, M.; Takayama, H.; Muroi, M.; Kimura, S.; Maekawa, T.; Osada, H. *Chem. Biol.* **2011**, *18*, 743.
60. Young, D. W.; Bender, A.; Hoyt, J.; McWhinnie, E.; Chirn, G. W.; Tao, C. Y.; Tallarico, J. A.; Labow, M.; Jenkins, J. L.; Mitchison, T. J., et al *Nat. Chem. Biol.* **2008**, *4*, 59.
61. Li, L.; Wang, H. K.; Kuo, S. C.; Wu, T. S.; Mauger, A.; Lin, C. M.; Hamel, E.; Lee, K. H. *J. Med. Chem.* **1994**, *37*, 3400.
62. Shi, Q.; Chen, K.; Morris-Natschke, S. L.; Lee, K. H. *Curr. Pharm. Des.* **1998**, *4*, 219.
63. Tong, Y. G.; Zhang, X. W.; Geng, M. Y.; Yue, J. M.; Xin, X. L.; Tian, F.; Shen, X.; Tong, L. J.; Li, M. H.; Zhang, C., et al *Mol. Pharmacol.* **2006**, *69*, 1226.
64. Sumiya, E.; Shimogawa, H.; Sasaki, H.; Tsutsumi, M.; Yoshita, K.; Ojika, M.; Suenaga, K.; Uesugi, M. *ACS Chem. Biol.* **2011**, *6*, 425.
65. Flanagan, M. D.; Lin, S. *J. Biol. Chem.* **1980**, *255*, 835.
66. Bai, R.; Covell, D. G.; Liu, C.; Ghosh, A. K.; Hamel, E. *J. Biol. Chem.* **2002**, *277*, 32165.
67. Bubb, M. R.; Senderowicz, A. M.; Sausville, E. A.; Duncan, K. L.; Korn, E. D. *J. Biol. Chem.* **1994**, *269*, 14869.
68. Coue, M.; Brenner, S. L.; Spector, I.; Korn, E. D. *FEBS Lett.* **1987**, *213*, 316.
69. Saito, S.; Watabe, S.; Ozaki, H.; Fusetani, N.; Karaki, H. *J. Biol. Chem.* **1994**, *269*, 29710.
70. Tanaka, C.; Tanaka, J.; Bolland, R. F.; Marriott, G.; Higa, T. *Tetrahedron* **2006**, 62.
71. Bubb, M. R.; Spector, I.; Bershadsky, A. D.; Korn, E. D. *J. Biol. Chem.* **1995**, *270*, 3463.
72. Ojika, M.; Inukai, Y.; Kito, Y.; Hirata, M.; Iizuka, T.; Fudou, R. *Chem. Asian J.* **2008**, *3*, 126.
73. Iizuka, T.; Fudou, R.; Jojima, Y.; Ogawa, S.; Yamanaka, S.; Inukai, Y.; Ojika, M. *J. Antibiot. (Tokyo)* **2006**, *59*, 385.
74. Teruya, T.; Sasaki, H.; Fukazawa, H.; Suenaga, K. *Org. Lett.* **2009**, *11*, 5062.
75. Gao, X.; Liu, Y.; Kwong, S.; Xu, Z.; Ye, T. *Org. Lett.* **2010**, *12*, 3018.
76. Soga, T.; Ohashi, Y.; Ueno, Y.; Naraoka, H.; Tomita, M.; Nishioka, T. *J. Proteome Res.* **2003**, *2*, 488.
77. Monton, M. R.; Soga, T. *J. Chromatogr., A* **2007**, *1168*, 237. discussion 236.
78. Hirayama, A.; Kami, K.; Sugimoto, M.; Sugawara, M.; Toki, N.; Onozuka, H.; Kinoshita, T.; Saito, N.; Ochiai, A.; Tomita, M., et al *Cancer Res.* **2009**, *69*, 4918.
79. Ishii, N.; Nakahigashi, K.; Baba, T.; Robert, M.; Soga, T.; Kanai, A.; Hirasawa, T.; Naba, M.; Hirai, K.; Hoque, A., et al *Science* **2007**, *316*, 593.
80. Soga, T.; Baran, R.; Suematsu, M.; Ueno, Y.; Ikeda, S.; Sakurakawa, T.; Kakazu, Y.; Ishikawa, T.; Robert, M.; Nishioka, T., et al *J. Biol. Chem.* **2006**, *281*, 16768.
81. Sugimoto, M.; Wong, D. T.; Hirayama, A.; Soga, T.; Tomita, M. *Metabolomics* **2010**, *6*, 78.
82. Faix, J.; Rottner, K. *Curr. Opin. Cell Biol.* **2006**, *18*, 18.
83. Mattila, P. K.; Lappalainen, P. *Nat. Rev. Mol. Cell Biol.* **2008**, *9*, 446.
84. Kitagawa, M.; Ikeda, S.; Tashiro, E.; Soga, T.; Imoto, M. *Chem. Biol.* **2010**, *17*, 989.
85. Parsons, A. B.; Brost, R. L.; Ding, H.; Li, Z.; Zhang, C.; Sheikh, B.; Brown, G. W.; Kane, P. M.; Hughes, T. R.; Boone, C. *Nat. Biotechnol.* **2004**, *22*, 62.
86. Parsons, A. B.; Lopez, A.; Givoni, I. E.; Williams, D. E.; Gray, C. A.; Porter, J.; Chua, G.; Sopko, R.; Brost, R. L.; Ho, C. H., et al *Cell* **2006**, *126*, 611.
87. Ayscough, K. R.; Stryker, J.; Pokala, N.; Sanders, M.; Crews, P.; Drubin, D. G. *J. Cell Biol.* **1997**, *137*, 399.
88. Torralba, S.; Raudaskoski, M.; Pedregosa, A. M.; Laborda, F. *Microbiology* **1998**, *144*, 45.
89. Yoshida, S.; Ikeda, E.; Uno, I.; Mitsuzawa, H. *Mol. Gen. Genet.* **1992**, *231*, 337.
90. Douglas, C. M.; Marrinan, J. A.; Li, W.; Kurtz, M. B. *J. Bacteriol.* **1994**, *176*, 5686.
91. Roe, S. M.; Prodromou, C.; O'Brien, R.; Ladbury, J. E.; Piper, P. W.; Pearl, L. H. *J. Med. Chem.* **1999**, *42*, 260.
92. Gupta, S. S.; Ton, V. K.; Beaudry, V.; Rulli, S.; Cunningham, K.; Rao, R. *J. Biol. Chem.* **2003**, *278*, 28831.
93. Kitagawa, I.; Kobayashi, M.; Imamoto, T.; Yasuzawa, T.; Kyogoku, Y. *Chem. Pharm. Bull.* **1981**, *29*, 2387.
94. Schmidt, E. W.; Bewley, C. A.; Faulkner, D. J. *J. Org. Chem.* **1998**, *63*, 1254.
95. Nishimura, S.; Arita, Y.; Honda, M.; Iwamoto, K.; Matsuyama, A.; Shirai, A.; Kawasaki, H.; Kakeya, H.; Kobayashi, T.; Matsunaga, S., et al *Nat. Chem. Biol.* **2010**, *6*, 519.
96. Matsunaga, S.; Fusetani, N. *J. Org. Chem.* **1995**, *60*, 1177.
97. Matsunaga, S.; Fusetani, N.; Hashimoto, K.; Walchli, M. *J. Am. Chem. Soc.* **1989**, *111*, 2582.
98. Wada, S.; Matsunaga, S.; Fusetani, N.; Watabe, S. *Mar. Biotechnol. (NY)* **2000**, *2*, 285.
99. Matsuyama, A.; Arai, R.; Yashiroda, Y.; Shirai, A.; Kamata, A.; Sekido, S.; Kobayashi, Y.; Hashimoto, A.; Hamamoto, M.; Hiraoka, Y., et al *Nat. Biotechnol.* **2006**, *24*, 841.
100. Shirai, A.; Matsuyama, A.; Yashiroda, Y.; Hashimoto, A.; Kawamura, Y.; Arai, R.; Komatsu, Y.; Horinouchi, S.; Yoshida, M. *J. Biol. Chem.* **2008**, *283*, 10745.

THE JOURNAL OF BIOLOGICAL CHEMISTRY VOL. 286, NO. 45, pp. 39259–39268, November 11, 2011

Involvement of 14-3-3 Proteins in the Second Epidermal Growth Factor-induced Wave of Rac1 Activation in the Process of Cell Migration*[S]

Received for publication, April 27, 2011, and in revised form, August 11, 2011 Published, JBC Papers in Press, August 25, 2011, DOI 10.1074/jbc.M111.255489

Hiroki Kobayashi[‡], Yusuke Ogura[§], Masato Sawada[‡], Ryoji Nakayama[‡], Kei Takano[‡], Yusuke Minato[‡], Yasushi Takemoto[‡], Etsu Tashiro[‡], Hidenori Watanabe[§], and Masaya Imoto[‡1]

From the [‡]Department of Biosciences and Informatics, Faculty of Science and Technology, Keio University, 3-14-1 Hiyoshi, Kohoku-ku, Yokohama 223-8522, Japan and the [§]Graduate School of Agricultural and Life Sciences, The University of Tokyo, 1-1-1 Yayoi, Bunkyo-ku, Tokyo 113-8657, Japan

Background: The spatiotemporal regulation of Rac1 controls cell migration.
Results: EGF induced two waves of Rac1 activation in the process of cell migration.
Conclusion: 14-3-3 proteins regulate the second EGF-induced wave of Rac1 activation by interacting with RacGEF.
Significance: The second wave of Rac1 activation might be required for EGF-induced cell migration.

Immense previous efforts have elucidated the core machinery in cell migration, actin remodeling regulated by Rho family small GTPases including RhoA, Cdc42, and Rac1; however, the spatiotemporal regulation of these molecules remains largely unknown. Here, we report that EGF induces biphasic Rac1 activation in the process of cell migration, and UTKO1, a cell migration inhibitor, inhibits the second EGF-induced wave of Rac1 activation but not the first wave. To address the regulation mechanism and role of the second wave of Rac1 activation, we identified 14-3-3ζ as a target protein of UTKO1 and also showed that UTKO1 abrogated the binding of 14-3-3ζ to Tiam1 that was responsible for the second wave of Rac1 activation, suggesting that the interaction of 14-3-3ζ with Tiam1 is involved in this event. To our knowledge, this is the first report to use a chemical genetic approach to demonstrate the mechanism of temporal activation of Rac1.

The importance of cell migration is evident from the number of physiological processes that depend on the regulated movement of cells, including embryonic development, immune responses, and tissue maintenance and repair, and also from the disease states driven by aberrant cell motility, such as chronic inflammation, vascular disease, and tumor metastasis (1). Key to the capacity of the cell to migrate is dynamic reorganization of the actin cytoskeleton (2). When a cell moves, site-directed *de novo* nucleation and polymerization of actin drives protrusive membrane structures such as lamellipodia and filopodia, which generate the locomotive force in migrating cells (3, 4). Reorganization of the actin cytoskeleton is regulated by actin-nucleating factors, the most prominent of which is the Arp2/3 complex (5). Catalytic activation of this complex is mediated by WASP/WAVE family members, which in turn translate extracellular signals via the Rho family of small GTPases such as RhoA, Cdc42, and Rac1 (6). In particular, activation of RhoA increases cell contractility and leads to the formation of focal adhesions and stress fibers (7). Activation of Cdc42 and Rac1 propagates the formation of filopodia and lamellipodia, respectively (8, 9).

The Rho family GTPases function as binary switches that cycle between an active GTP-bound form and an inactive GDP-bound form. This cycling is regulated through three factors: guanine nucleotide exchange factor (GEF),[2] GTPase-activating protein, and guanine nucleotide dissociation inhibitor (10, 11). Among them, GEF activates the Rho family GTPases by promoting the exchange of GDP with GTP, resulting in the binding of the GTPases to their effectors. A number of GEFs have been shown to transduce signals from many growth factors to the Rho family GTPases. In addition to the increasing number of GEFs, the redundant specificity of GEFs renders signaling networks controlling cell migration difficult to understand; many GEFs have been shown to take multiple Rho family GTPases as substrates, at least *in vitro* (11, 12). The spatiotemporal coordination of the Rho family GTPases by these molecules regulates a complicated dynamic process of cell migration.

Inhibitors of cell migration would be useful not only as tools for basic research into cell migration but also as anti-metastatic drug-leads for cancer therapy. To obtain cell migration inhibitor, UTKO1 was synthesized as a derivative of natural products moverastins, which inhibit migration of EC17 cells by inhibiting farnesylation of H-Ras (13). However, although its chemical structure is very similar to that of moverastins, its inhibitory effect on cell migration was stronger than that of the moverastins and did not involve inhibition of farnesyltransferase (14). UTKO1 also failed to inhibit MEK/ERK and the PI3K/Akt path-

* This work was supported by a grant from the Ministry of Education, Culture, Sports, Science, and Technology.
[S] The on-line version of this article (available at http://www.jbc.org) contains supplemental text, Scheme S1, and Figs. S1–S9.
[1] To whom correspondence should be addressed: Dept. of Biosciences and Informatics, Faculty of Science and Technology, Keio University, 3-14-1 Hiyoshi, Kohoku-ku, Yokohama 223-8522, Japan. Tel./Fax: 81-45-566-1557; E-mail: imoto@bio.keio.ac.jp.

[2] The abbreviations used are: GEF, guanine nucleotide exchange factor; IP, immunoprecipitation; CBB, Coomassie Brilliant Blue; EGF, epidermal growth factor.

way generally known to regulate cell migration.[3] This unique pharmacological profile of UTKO1 has drawn considerable interest, prompting us to further investigate its mechanism of action. In this report, we present evidence that EGF induces two waves of Rac1 activation in the process of cell migration and that UTKO1 inhibited only the second of these waves by targeting 14-3-3ζ. Furthermore, we showed that UTKO1 abrogated the binding of 14-3-3ζ to Tiam1 that was responsible for the second wave of Rac1 activation, presumably resulting in the inhibition of EGF-induced cell migration.

EXPERIMENTAL PROCEDURES

DNA Constructs—Human cDNA for 14-3-3s (α/β, ε, η, γ, τ/θ, ζ/δ, and σ) were amplified from HeLa cell cDNA and cloned into pcDNA3 (Invitrogen, San Diego, CA) with the N-terminal FLAG tag. All of the constructs were cloned into pGEX-2T (GE Healthcare, Princeton, NJ) to prepare GST fusion proteins in bacteria. Expression vectors encoding GST-fused 14-3-3ζ mutants (ΔC100, 1–145 amino acids; ΔC200, 1–45 amino acids; and C50, 196–245 amino acids) were generated by PCR using pGEX-2T/14-3-3ζ as a template. pCS2+MT/Tiam1, a expression vector encoding human Tiam1 followed by 6×Myc, was kindly provided by Dr. H. Sugimura (Hamamatsu University School of Medicine, Hamamatsu, Japan).

Chemotaxis Chamber Assay—Cell migration was assayed with a chemotaxis chamber (Becton Dickinson, Franklin Lakes, NJ). A431 cells suspended in DMEM supplemented with 0.2% calf serum were incubated in the upper chamber; the lower chamber contained DMEM supplemented with 0.2% calf serum in the presence or absence of EGF (30 ng/ml). Drugs were added to both chambers. Following 24 h of incubation, the filter was fixed with MeOH and stained with hematoxylin (Sigma, St. Louis, MO). The cells attached to the lower side of the filter were counted.

Confocal Laser Scanning Microscopy—Cells were fixed with 3% paraformaldehyde for 15 min and permeabilized with 0.5% Triton X-100 in PBS for 5 min. After rinsing three times with PBS, the cells were incubated in blocking buffer (1% bovine serum albumin in PBS) for 30 min then stained with Texas Red®-X phalloidin (1:100; Molecular Probes, Eugene, OR) at room temperature for 1 h. Fluorescence images were obtained using a confocal laser scanning microscope system FV1000 (Olympus, Tokyo, Japan). Lamellipodia formation (%) means the ratio of the number of cells with lamellipodia in the total cell count.

Detection of Active Rac1—The cells were lysed with magnesium-containing lysis buffer (25 mM HEPES, pH 7.5, 150 mM NaCl, 1% Nonidet P-40, 0.25% sodium deoxycholate, 10% glycerol, 25 mM NaF, 10 mM $MgCl_2$, 1 mM EDTA, 1 mM Na_3VO_4, and a protease inhibitor mixture (Roche Applied Science)). The cell lysates were cleared by centrifugation at 15,000 × *g* for 10 min at 4 °C. Pak1 PBD-agarose (Millipore, Bedford, MA) was incubated with the lysates at 4 °C for 1 h and washed three times with magnesium-containing lysis buffer, and then active Rac1 was eluted by boiling in SDS sample buffer for 5 min. The resultant samples were subjected to Western blotting.

Identification of B-UTKO1 Binding Proteins—A431 cells were stimulated with EGF (30 ng/ml) for 4 h. The cells were collected and sonicated twice in immunoprecipitation (IP) buffer (50 mM HEPES, pH 7.5, 150 mM NaCl, 2.5 mM EGTA, 1 mM EDTA, 1 mM DTT, and a protease inhibitor mixture) for 10 s. The cell lysates were centrifuged at 130,000 × *g* for 1 h at 4 °C. The resulting supernatant was precleared twice with avidin beads (Pierce) for 1 h and incubated with biotin (50 nmol) or B-UTKO1ox (50 nmol) and avidin beads at 4 °C overnight. The beads were washed three times with IP buffer and once with PBS. The bound proteins were eluted with 2 mM biotin in PBS and concentrated by a centrifugal filter device (Ultracel (YM-10); Millipore). The resulting proteins were subjected to SDS-PAGE followed by Coomassie Brilliant Blue (CBB) staining (see Fig. 3*B*) or immunoblotting (see Fig. 4*A*). Following CBB staining, the bands corresponding to the UTKO1 binding proteins were excised, and the gel pieces were destained with 50% CH_3CN in 50 mM NH_4HCO_3 solution. After removal of the supernatant, cysteine residues were reduced with DTT, carbamidomethylated with indoacetamide, and the proteins were digested with trypsin at 37 °C overnight. The tryptic peptides were recovered by sequentially adding three solvent systems containing 50% CH_3CN and 1% TFA; 20% HCOOH, 25% CH_3CN and 15% *i*-PrOH; and 80% CH_3CN. The supernatants were collected and pooled into one tube, reducing the volume *in vacuo*. The dried tryptic peptides were suspended in 2% CH_3CN and 0.1% TFA and applied to the following LC-MS/MS system. Chromatographic separation was accomplished with the MAGIC 2002 HPLC system (Michrom BioResources). Peptide samples were loaded onto a Cadenza C18 custom-packed column (0.2 × 50 mm; Michrom BioResources) and eluted using a linear gradient of 5–60% CH_3CN in 0.1% HCOOH for 30 min at a flow rate of 1 ml/min. Samples were ionized with a Nanoflow-LC ESI, and MS/MS spectrum data were obtained with an LCQ-Deca XP ion trap mass spectrometer (Thermo Electron). The Mascot data base searching software (Matrix Science) was used for the identification of B-UTKO1ox binding proteins.

Immunoprecipitation—A431/FLAG-14-3-3ζ cells were transiently transfected with pCS2+MT/Tiam1 using Metafectene Pro (Biontex, Munich, Germany). Following 24 h of transfection, the cells were pretreated with UTKO1 for 15 min and stimulated with EGF for 12 h. The cells were collected and sonicated in IP buffer. The cell lysates were cleared by centrifugation at 15,000 × *g* for 15 min at 4 °C then incubated with anti-FLAG antibody and protein A/G-agarose beads (Santa Cruz, Santa Cruz, CA) at 4 °C overnight. The immunoprecipitants were washed once with IP buffer and twice with IP buffer containing 1% Nonidet P-40. The bound proteins were eluted by boiling in SDS sample buffer for 5 min and subjected to Western blotting.

In Vitro B-UTKO1 Pulldown Assay—GST fusion proteins, which were expressed in the *Escherichia coli* DH5α strain and purified using glutathione-Sepharose 4B (GE Healthcare), were incubated with B-UTKO1ox and avidin beads in 500 μl of IP

[3] S. Magi and M. Imoto, unpublished observations.

buffer for 3 h. The beads were washed and eluted with 2 mM biotin in PBS. The eluted proteins were subjected to SDS-PAGE. For the competition assay, UTKO1 was added before incubating with B-UTKO1ox.

GST Pulldown Assay—The collected cells were sonicated twice in IP buffer for 10 s. The cell lysates were cleared by centrifugation at 15,000 × *g* for 15 min at 4 °C and then incubated with purified GST or GST-14-3-3ζ and glutathione-Sepharose 4B (GE Healthcare) for 2 h. The bound proteins were eluted by boiling in SDS sample buffer for 5 min and subjected to Western blotting. For Fig. 6*A*, purified GST-14-3-3ζ was pre-incubated with UTKO1 in a total volume of 1 ml of IP buffer for 1 h. Other experimental procedures are given in the supplemental materials.

RESULTS

UTKO1 Inhibits the Second EGF-induced Wave of Lamellipodia Formation—The formation of lamellipodia, protruding membrane structures at the leading edge of migrating cells, is key in cell migration (15). We observed transient lamellipodia formation at 5 min following EGF stimulation, as reported elsewhere (12, 16), and we also found a second wave of lamellipodia formation to be initiated at 6–9 h and reach its zenith within 12 h after EGF stimulation in human epidermoid carcinoma A431 cells (Fig. 1, *A* and *B*). Furthermore, we found that UTKO1 (Fig. 1*C*), a cell migration inhibitor (14), inhibited only the second wave of that as shown in Fig. 1 (*D–G*); we evaluated the effect of UTKO1 on the lamellipodia formation induced by treatment with EGF for 5 min and for 12 h, respectively, and found no inhibition of lamellipodia formation at 5 min; lamellipodia formation at 12 h was inhibited by UTKO1 with an IC_{50} value of 0.78 μM. This IC_{50} value is almost the same as that for inhibiting cell migration (0.67 μM; Fig. 1*H*). Similar results were obtained when TT cells, a human esophageal cancer cell line, were used in place of A431 cells (supplemental Fig. S1). Thus, although EGF induced two waves of lamellipodia formation, at 5 min and 12 h after stimulation, UTKO1 inhibited only the second wave.

UTKO1 Inhibits the Second EGF-induced Wave of Rac1 Activation—Lamellipodia formation has been reported to be mainly regulated by Rac1, a member of the Rho family of small GTPases (9, 17). Because lamellipodia formation was observed at 5 min and 12 h following EGF stimulation, we next examined whether EGF also induces two waves of Rac1 activation. Rac1 was rapidly and transiently activated at 2–5 min after EGF stimulation, as expected from previous published reports (12, 18), and we also found that active Rac1 began to increase from 6 h onward. This second wave of Rac1 activation was much broader than the first wave and lasted until 12 h after EGF stimulation (Fig. 2*A*). UTKO1 did not inhibit the first wave of Rac1 activation even when the cells were pretreated with UTKO1 for 12 h but did inhibit the second wave (Fig. 2, *B* and *C*). Similar results were obtained when TT cells were used in place of A431 cells (supplemental Fig. S2). Moreover, when UTKO1 was added at 4 h after EGF stimulation, the second EGF-induced wave of Rac1 activation, lamellipodia formation, and cell migration were all inhibited (Fig. 2, *D–F*). These results indicate that UTKO1 suppresses EGF-induced cell migration, possibly via inhibition of the second wave of Rac1 activation required for lamellipodia formation.

Identification of 14-3-3ζ as a UTKO1-binding Protein—To elucidate the mechanism for the inhibition of cell migration caused by UTKO1, we tried to identify the target protein of UTKO1 responsible for Rac1 activation at 12 h following EGF stimulation. We used biotinylated UTKO1s (B-UTKO1ox and B-UTKO1ph) (Fig. 3*A* and supplemental Scheme S1), which were biologically active with the same potency as UTKO1. Lysates of A431 cells stimulated with EGF for 4 h were incubated overnight with B-UTKO1ox and avidin beads. The B-UTKO1ox-bound avidin beads were precipitated and washed, and co-precipitated proteins were eluted by excess biotin. The eluted proteins were separated by SDS-PAGE and detected by CBB staining (Fig. 3*B*). We observed 10 major protein bands that specifically co-precipitated with B-UTKO1oxand identified these proteins by LC-MS/MS system as: 1) GRP78; 2) PDI; 3) nucleobindin-2; 4) 2-phosphopruvate-hydratase α-enolase; 5) unnamed product; 6) unnamed product; 7) mutant β-actin; 8) annexin A2; 9) 14-3-3ε; and 10) 14-3-3ζ. The peptide sequences of unnamed products 5 and 6 suggest them to be nuclear lamin proteins. Of these 10 proteins, we speculated that 14-3-3ζ might be the target of UTKO1, because it has been previously reported to relate to the formation of lamellipodia (19, 20). The binding of UTKO1 to 14-3-3ζ was confirmed by Western blotting of B-UTKO1ox- or B-UTKO1ph-bound proteins using anti-14-3-3ζ antibody, as shown in Fig. 4*A*. Next, to determine whether UTKO1 could bind directly to 14-3-3ζ, we performed *in vitro* B-UTKO1 pulldown experiments using purified GST-tagged 14-3-3ζ. GST-14-3-3ζ co-precipitated with B-UTKO1ox: competition was clearly observed in the presence of UTKO1 (Fig. 4*B*). These results suggest that UTKO1 binds directly to 14-3-3ζ. Moreover, we found that B-UTKO1ox did not bind to a C terminus deletion mutant of 14-3-3ζ, indicating that the binding of UTKO1 to 14-3-3ζ is probably via the C-terminal region (supplemental Fig. S3). 14-3-3ζ is a member of the 14-3-3 family, and at least seven different isoforms have been identified in mammalian cells (21, 22). Therefore, we prepared seven recombinant GST-14-3-3 isoforms and performed *in vitro* B-UTKO1 pulldown experiments to test each for its ability to bind to UTKO1. As a result, the ζ isoform showed the strongest binding ability to B-UTKO1ox (Fig. 4*C*).

Next, we performed RNAi experiments to investigate whether the loss of 14-3-3ζ could suppress EGF-induced cell migration, lamellipodia formation, and Rac1 activation in A431 cells. The successful knockdown of 14-3-3ζ by siRNA was confirmed by Western blotting (Fig. 4*D*). Silencing of 14-3-3ζ expression consequently suppressed EGF-induced cell migration in A431 cells (Fig. 4*E*). Furthermore, silencing of 14-3-3ζ expression did not inhibit EGF-induced Rac1 activation at 2 min and lamellipodia formation at 5 min but did inhibit both EGF-induced Rac1 activation and lamellipodia formation at 12 h, as shown in Fig. 4 (*F–H*). These results indicate that 14-3-3ζ acts upstream of the second EGF-induced wave of Rac1 activation. Additionally, EGF-induced filopodia-like structures observed in 14-3-3ζ knockdown A431 cells (Fig.

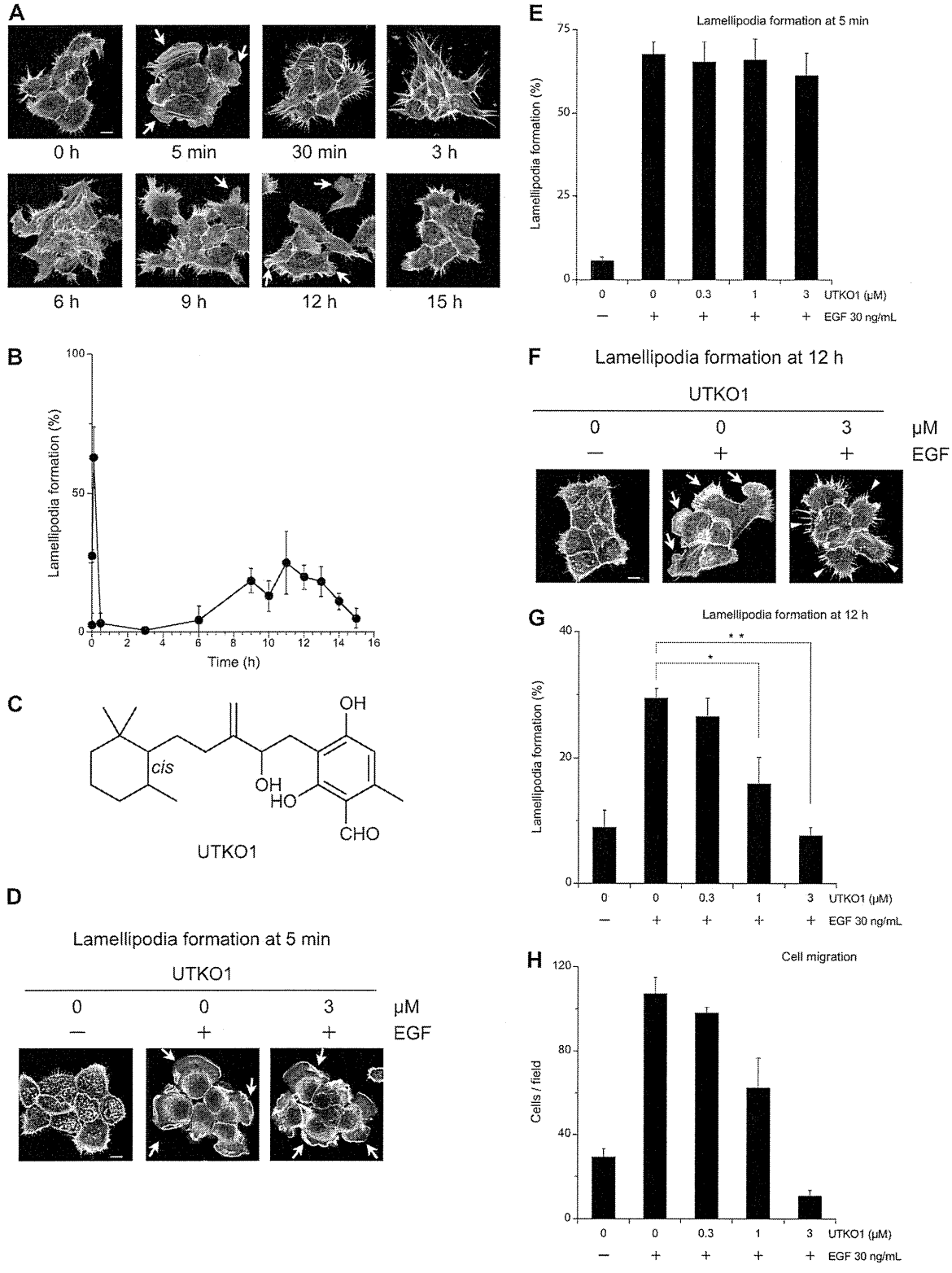

FIGURE 1. **UTKO1 inhibits the second EGF-induced wave of lamellipodia formation in A431 cells.** *A* and *B*, EGF-induced lamellipodia formation in A431 cells, observed under confocal microscopy (*A*) and counted (*B*). *C*, structure of UTKO1. *D–G*, effect of UTKO1 on EGF-induced lamellipodia formation. A431 cells were pretreated with the indicated concentrations of UTKO1 for 15 min and stimulated with EGF. After 5 min (*D* and *E*) or 12 h (*F* and *G*), the cells were observed under confocal microscopy (*D* and *F*) and counted (*E* and *G*). The data represent the means ± S.D. ($n = 6$). *H*, inhibitory activity of UTKO1 on EGF-induced cell migration, monitored using a chemotaxis chamber. The data represent the means ± S.D. ($n = 5$). Throughout, the data were representative of at least three independent studies. *Arrows*, lamellipodia; *arrowheads*, see text. *Scale bar*, 10 μm. For *G*, statistical analyses were performed with a two-tailed Student's *t* test. *, $p = 0.00013$; **, $p = 1.0 \times 10^{-5}$. For *B*, *E*, and *G*, more than 300 cells were analyzed per experiment.